The Iron Isotope Fingerprints of Redox and Biogeochemical Cycling in Modern and Ancient Earth

Clark M. Johnson, Brian L. Beard, and Eric E. Roden

NASA Astrobiology Institute and Department of Geology and Geophysics, University of Wisconsin, Madison, Wisconsin 53706; email: clarkj@geology.wisc.edu, beardb@geology.wisc.edu, eroden@geology.wisc.edu

Annu. Rev. Earth Planet. Sci. 2008. 36:457–93

The *Annual Review of Earth and Planetary Sciences* is online at earth.annualreviews.org

This article's doi:
10.1146/annurev.earth.36.031207.124139

0084-6597/08/0530-0457$20.00

Key Words

Precambrian, life, evolution, diagenesis

Abstract

The largest Fe isotope fractionations occur during redox changes, as well as differences in bonding, but these are expressed only in natural environments in which significant quantities of Fe may be mobilized and separated. At the circumneutral pH of most low-temperature aqueous systems, Fe^{2+}_{aq} is the most common species for mobilizing Fe, and Fe^{2+}_{aq} has low $^{56}Fe/^{54}Fe$ ratios relative to Fe^{3+}-bearing minerals. Of the variety of abiologic and biologic processes that involve redox or bonding changes, microbial Fe^{3+} reduction produces the largest quantities of isotopically distinct Fe by several orders of magnitude relative to abiologic processes and hence plays a major role in producing Fe isotope variations on Earth. In modern Earth, the mass of Fe cycled through redox boundaries is small, but in the Archean it was much larger, reflecting juxtaposition of large inventories of Fe^{2+} and Fe^{3+}. Development of photosynthesis produced large quantities of Fe^{3+} and organic carbon that fueled a major expansion in microbial Fe^{3+} reduction in the late Archean, perhaps starting as early as ~3 Ga. The Fe isotope fingerprint of microbial Fe^{3+} reduction decreases in the sedimentary rock record between ~2.4 and 2.2 Ga, reflecting increased bacterial sulfate reduction and a concomitant decrease in the availability of reactive iron to support microbial Fe^{3+} reduction. The temporal C, S, and Fe isotope record therefore reflects the interplay of changing microbial metabolisms over Earth's history.

INTRODUCTION

Some two-dozen laboratories worldwide are pursuing Fe isotope research across a variety of topics, ranging from studying human blood (e.g., Walczyk & von Blanckenburg 2002), tracing Fe pathways in the modern oceans (e.g., Levasseur et al. 2004), determining redox cycling in ancient Earth (e.g., Rouxel et al. 2005), to studying solar system differentiation (e.g., Poitrasson et al. 2004). A decade ago only a few abstracts had been published on Fe isotope geochemistry, reflecting analytical development efforts that began in the mid-1990s (Beard et al. 1998, Bullen & McMahon 1998). Although these early efforts were significantly limited in the quantity and quality of data they could obtain, they were motivated by a desire to develop new tools for understanding the biological cycling of Fe, specifically microbial Fe^{3+} reduction, which was recognized in the late 1980s as a major process by which Fe is cycled in the surface environments of Earth (Lovley & Phillips 1988, Myers & Nealson 1988). The proposal that Fe isotopes may be a biosignature for microbial Fe cycling (Beard et al. 1999), however, was greeted with skepticism (Anbar et al. 2000, Bullen et al. 2001), and in the early 2000s, we saw a rapid increase in experimental and theoretical studies into the mechanisms of Fe isotope fractionation in abiologic and biologic systems (e.g., Polyakov & Mineev 2000, Brantley et al. 2001, Schauble et al. 2001, Johnson et al. 2002). Since this time, the pace of investigations has only quickened.

There have been a number of reviews on Fe isotope geochemistry in the past several years (Anbar 2004, Beard & Johnson 2004, Johnson et al. 2004, Dauphas & Rouxel 2006, Johnson & Beard 2006, Anbar & Rouxel 2007). These reviews have been split in terms of the role of biogeochemical cycling in determining the Fe isotope record of Earth, with some preferring abiological processes to explain the data (e.g., Dauphas & Rouxel 2006, Anbar & Rouxel 2007) and others highlighting the role that the microbial processing of Fe has had on the isotopic record (e.g., Johnson et al. 2004, Johnson & Beard 2006). Abiologic processes such as extensive $Fe^{2+}{}_{aq}$ oxidation have been proposed to explain the large range in Fe isotope compositions observed in Archean sedimentary rocks (e.g., Rouxel et al. 2005), but we show below that such processes produce two to three orders of magnitude smaller quantities of fractionated Fe relative to those produced by microbial Fe^{3+} reduction. We review data on natural systems and experiments, looking at both abiological and biological processes, where the ultimate goal is to understand the isotopic fingerprints of the C, S, and Fe biogeochemical cycles over Earth's history, and assessing how these fingerprints may reflect changing microbial metabolisms and environmental conditions.

ISOTOPIC FRACTIONATION

All data discussed here are reported as δ^{56}Fe values, in units of per mil (‰), relative to the average of igneous rocks (Beard et al. 2003a):

$$\delta^{56}\mathrm{Fe} = ({}^{56}\mathrm{Fe}/{}^{54}\mathrm{Fe}_{\mathrm{Sample}}/{}^{56}\mathrm{Fe}/{}^{54}\mathrm{Fe}_{\mathrm{Ig\ Rxs}} - 1)^{*}10^{3}. \quad (1)$$

The precision of δ^{56}Fe values is generally ± 0.05‰ to ± 0.15‰, depending on the laboratory. Following standard practice, we describe isotopic fractionations between

two components, A and B, by the isotopic fractionation factor, α_{A-B}:

$$\alpha_{A-B} = (^{56}Fe/^{54}Fe)_A/(^{56}Fe/^{54}Fe)_B. \quad (2)$$

For isotopic systems in which fractionations are on the order of a few per mil (as is the case for Fe), we can employ a useful approximation:

$$10^3 \ln\alpha_{A-B} \approx \delta^{56}Fe_A - \delta^{56}Fe_B = \Delta^{56}Fe_{A-B}. \quad (3)$$

The general principles of stable isotope fractionation can be found in numerous textbooks (e.g., Criss 1999), and discussions oriented toward transition-metal isotope systems may be found in Schauble (2004) and Anbar & Rouxel (2007).

The most important controls on Fe isotope fractionations in natural, low-temperature systems are oxidation state and bonding. Under equilibrium conditions, aqueous Fe or minerals that are entirely Fe^{3+} have higher $\delta^{56}Fe$ values than those of mixed Fe^{3+}-Fe^{2+} oxidation state, and aqueous species or minerals that are entirely Fe^{2+} tend to have the lowest $\delta^{56}Fe$ values; exceptions to these general trends include aqueous species or minerals in which Fe is covalently bonded such as pyrite, which is predicted to have some of the highest $\delta^{56}Fe$ values of minerals that occur in sedimentary rocks (e.g., Polyakov & Mineev 2000). When these guidelines do not appear to be observed in natural systems, the most likely explanation is that nonequilibrium, pathway-dependent processes are responsible. Reviews of Fe isotope fractionation factors may be found in Beard & Johnson (2004), Johnson et al. (2004, 2005), Anbar & Rouxel (2007), and Polyakov et al. (2007).

ISOTOPIC COMPOSITON OF THE BULK CRUST

The vast majority of Fe in the crust has a $\delta^{56}Fe$ value near zero, including most igneous rocks, as well as most alteration and weathering products. Although surface weathering of most crustal lithologies under an O_2-bearing atmosphere produces large increases in Fe^{3+}/Fe^{2+} ratios and the formation of secondary silicate and oxide minerals that are relatively insoluble in neutral-pH solutions, the low solubility of Fe^{3+}-bearing minerals produces little net Fe isotope fractionation in bulk weathering products because loss of soluble Fe is insignificant (Beard et al. 2003b). Although slightly more variable in Fe isotope compositions, low-C, low-S Proterozoic and Archean shales also have $\delta^{56}Fe$ values that closely cluster around the igneous rock average (Yamaguchi et al. 2005). This result may at first seem surprising because weathering in the Archean is generally thought to have occurred prior to the development of an O_2-bearing atmosphere (e.g., Holland 1984). Weathering under an anoxic atmosphere, however, produces no redox change because the vast majority of Fe contained in igneous and metamorphic rocks is Fe^{2+}. Bulk sedimentary detritus therefore has $\delta^{56}Fe$ values near zero, independent of atmospheric O_2 contents (Yamaguchi et al. 2005). Collectively, these observations provide a powerful reference line over Earth's history (Archean to present) with which to compare rocks in which significant Fe was mobilized.

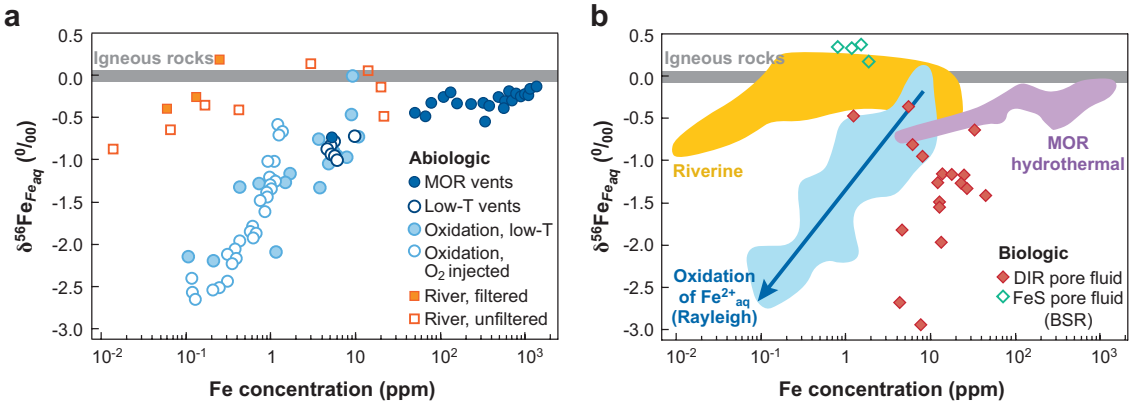

Figure 1

Variations in δ^{56}Fe values and Fe contents for aqueous Fe from natural fluids. Mafic igneous rocks have δ^{56}Fe values that lie between −0.1‰ and +0.1‰ (Beard et al. 2003a, Poitrasson et al. 2004). (*a*) Mid-ocean ridge (MOR) hydrothermal fluids, riverine Fe, low-temperature (low-T) hot springs, and groundwater that was injected with O_2. Data from Bullen et al. 2001; Beard et al. 2003b; Fantle & DePaolo 2004; Severmann et al. 2004; Poulson 2005; Teutsch et al. 2005; Bergquist & Boyle 2006; and S. Severmann, C. Johnson, B. Beard, and C. German, unpublished data. (*b*) Pore fluids from modern marine sediments from the California margin; data divided into samples in which the δ^{56}Fe values for Fe^{2+}_{aq} are controlled by dissimilatory iron reduction (DIR) and those controlled by exchange with FeS [ultimately related to bacterial sulfate reduction (BSR)]. Fields from panel *a* are shown for comparison. Trend for oxidation of Fe^{2+}_{aq} (Rayleigh process) shown by solid blue arrow. Data from Bergquist & Boyle 2006 and Severmann et al. 2006.

MOBILIZING IRON: ISOTOPIC VARIATIONS IN NATURAL FLUIDS

The isotopic homogeneity of most Fe reservoirs on Earth indicates that when nonzero δ^{56}Fe values are measured for minerals and rocks, they must have been produced by interactions with Fe-bearing fluids. Modern mid-ocean ridge hydrothermal fluids have δ^{56}Fe values between −0.8‰ and −0.1‰, and are positively correlated with Fe contents (**Figure 1*a***), indicating that their mass-weighted δ^{56}Fe value lies closer to the high end of this range. The higher heat flow in the Archean probably produced a mid-ocean-ridge hydrothermal flux that had a δ^{56}Fe value near zero (Yamaguchi et al. 2005, Johnson et al. 2008). The low-Fe fluids that have negative δ^{56}Fe values may be produced by precipitation of secondary minerals such as pyrite or oxides, which have δ^{56}Fe values higher than Fe^{2+}_{aq}.

The range in Fe isotope compositions measured for low-temperature fluids in diagenetic systems significantly exceeds that measured for mid-ocean-ridge hydrothermal fluids (**Figure 1**), as expected based on the general temperature dependence of isotopic fractionation factors. Four fundamental processes are reflected in the δ^{56}Fe-Fe concentration relations for low-temperature fluids: (*a*) the transport of dissolved or colloidal Fe in riverine systems, (*b*) the oxidation of Fe^{2+}_{aq}, (*c*) isotopic exchange

with reactive Fe monosulfide during bacterial sulfate reduction (BSR), and (*d*) isotopic fractionation associated with dissimilatory iron reduction (DIR) that is coupled to the bacterial oxidation of organic carbon (**Figure 1**).

Riverine Iron

The modern dissolved or colloidal riverine Fe flux appears to have slightly negative δ^{56}Fe values between zero and −1‰ (Fantle & DePaolo 2004, Bergquist & Boyle 2006), reflecting mobile Fe components that have been leached from soils during weathering, including colloidal oxides and Fe complexed by organic matter (Brantley et al. 2001, 2004; Fantle & DePaolo 2004; Emmanuel et al. 2005). The dissolved or colloidal riverine flux to the open oceans is $\sim 3 \times 10^9$ mol Fe per year, much smaller than the detrital or suspended load, which is approximately 1.2 to 1.8 $\times$ 10^{13} mol Fe per year (Poulton & Raiswell 2002). If the dissolved riverine Fe flux was greater in early Earth (under relatively anoxic conditions), the δ^{56}Fe values of this flux were probably close to zero, reflecting a higher degree of dissolution of igneous and metamorphic silicate minerals and the absence of significant redox changes upon weathering (Yamaguchi et al. 2005).

Oxidation of Ferrous Iron

Oxidation of Fe^{2+}_{aq} and precipitation of Fe^{3+} hydroxides (e.g., ferrihydrite) in groundwater or hot spring systems may produce δ^{56}Fe values for the remaining aqueous Fe^{2+} that are substantially lower than those measured for riverine Fe (**Figure 1**). Data are available for three systems: (*a*) Chocolate Pots Hot Springs, Yellowstone National Park (Poulson 2005), (*b*) spring water from Mt. Ruapehu, New Zealand (Bullen et al. 2001), and (*c*) a push-pull experiment in which O_2 was injected into reduced groundwater (Teutsch et al. 2005). At both Chocolate Pots and Mt. Ruapehu, moderate-temperature ($\leq$50°C) vent fluids are oxidized upon contact with the atmosphere, and the broadly linear trend of decreasing δ^{56}Fe with the logarithm of Fe concentration suggests a Rayleigh process (**Figure 1**). The changes in δ^{56}Fe for Fe^{2+}_{aq} are interpreted to reflect oxidation and precipitation in which the initial ferrihydrite-Fe^{2+}_{aq} fractionation factor was $\sim$+1‰, reflecting a combination of equilibrium isotope exchange between Fe^{3+}_{aq} and Fe^{2+}_{aq} ($\Delta^{56}Fe_{Fe^{3+}_{aq}-Fe^{2+}_{aq}} = +3.0‰$) and a kinetic fractionation upon precipitation ($\Delta^{56}Fe_{Fe(OH)_3-Fe^{3+}_{aq}} = -2.0‰$) (Beard & Johnson 2004), although the trends at both sites deviate from simple Rayleigh behavior at the greatest distances from the vent.

The potential role of sorption in determining the δ^{56}Fe values of aqueous Fe has received attention (e.g., Icopini et al. 2004). Partial dissolution of ferric hydroxide from Chocolate Pots shows that the most easily dissolved component has low-δ^{56}Fe values, opposite to what would be produced by Fe^{2+} sorption (Poulson 2005). The effects of sorption, however, are inferred to be the major control on the δ^{56}Fe values for Fe^{2+}_{aq} in Teutsch and colleagues' (2005) groundwater O_2 injection experiment. They argued that the homogenous oxidation of Fe^{2+}_{aq} during O_2 injection did not occur

and instead interpreted the results to indicate an equilibrium Fe isotope fractionation upon sorption of Fe^{2+}_{aq} onto newly formed ferric oxide/hydroxides. Alternatively, the formation of new oxide/hydroxides imparts an Fe isotope fractionation in which the remaining Fe^{2+}_{aq} has negative δ^{56}Fe values. The equilibrium Fe^{2+}_{aq}-Fe^{2+}_{sorb} fractionation at room temperature is relatively small and appears to be −0.9‰ and −0.3‰ for goethite and hematite, respectively, in both biologic (Crosby et al. 2005, 2007) and abiologic (Kennedy et al. 2006) experiments. These fractionations are far from the very large fractionations of 2‰ to 5‰ inferred (but not directly measured) by Icopini et al. (2004). The equilibrium Fe^{2+}_{aq}-Fe^{2+}_{sorb} fractionation for ferrihydrite has not been measured. Given the similarity in δ^{56}Fe-Fe concentration trends of the data from the groundwater experiment and the hot springs, we suggest that the oxidation of Fe^{2+}_{aq} and formation of new ferric oxide/hydroxides were more important controls on the Fe isotope compositions in the O_2 injection experiment.

Interactions with Reactive Fe^{3+}: Microbial Sulfate and Iron Reduction

BSR and DIR produce δ^{56}Fe values for Fe^{2+}_{aq} that are quite distinct. BSR is a major pathway of organic-matter degradation in many marine sediments (e.g., Canfield et al. 1993a), and Severmann et al. (2006) indicate that the Fe isotope compositions of Fe^{2+}_{aq} in sulfide-rich sections of modern marine sediments have relatively high-δ^{56}Fe values and low-Fe contents (**Figure 1*b***), reflecting isotopic exchange with iron monosulfide. This contrasts with the low-δ^{56}Fe values for Fe^{2+}_{aq} produced by DIR. Both BSR and DIR may occur in the same sediment section, reflecting extensive cycling of Fe and S before they are ultimately sequestered in the rock record as pyrite (e.g., Canfield et al. 1993a,b; Thamdrup & Canfield 1996), linking these two metabolic pathways and providing an opportunity for a range in Fe isotope compositions in sedimentary pyrite.

Of all the processes illustrated in **Figure 1**, DIR produces the highest concentrations of Fe^{2+}_{aq} in natural fluids that have isotopic compositions that are distinct from the crustal average. In areas in which reactive Fe^{3+} is abundant and SO_4^{2-} contents are limited, DIR is the major pathway of organic-matter degradation in marine sediments (Lovley & Phillips 1987). Pore fluids from modern marine sediments from the California and Amazon continental margins have relatively high-Fe^{2+}_{aq} contents in sediment sections that have high reactive Fe^{3+} contents, supporting relatively high levels of DIR. These Fe^{2+}_{aq}-rich pore fluids have δ^{56}Fe values that extend down to −3.0‰ (**Figure 1*b***), which are interpreted to reflect isotopic fractionations during DIR (Bergquist & Boyle 2006, Severmann et al. 2006). Staubwasser et al. (2006) have also inferred an active role for DIR in Fe cycling in modern marine sediments based on isotopic compositions of reactive Fe components in sediments from the Arabian Sea.

Experimental Studies of Abiologic and Biologic Mineral Dissolution

The relations between Fe isotope composition and concentrations of natural fluids in **Figure 1** lead us to conclude that in low-temperature diagenetic systems, DIR

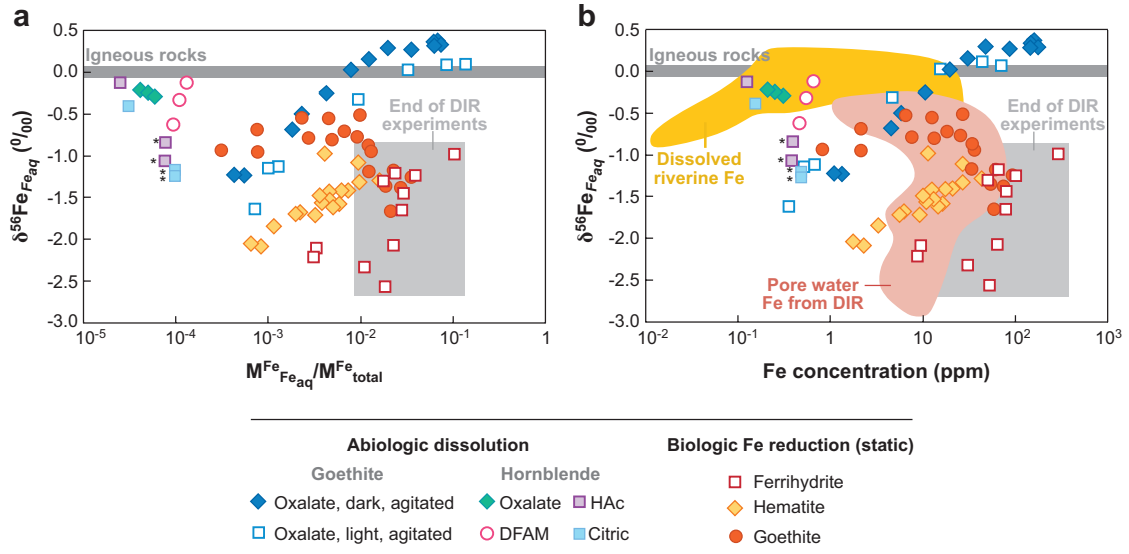

Figure 2

Iron isotope compositions for aqueous Fe from experimental studies of mineral dissolution in abiologic and biologic systems, relative to the molar fraction of aqueous Fe produced (fraction dissolved, panel *a*) and concentration of aqueous Fe (*b*). The Fe isotope compositions have been normalized to a system δ^{56}Fe value of zero. Experimental studies in panel *a* are shown for hornblende dissolution (Brantley et al. 2001, 2004), goethite dissolution by oxalate (Wiederhold et al. 2006), and dissimilatory iron reduction (DIR) of ferrihydrite, goethite, and hematite (Beard et al. 1999, 2003a; Icopini et al. 2004; Crosby et al. 2005, 2007; Johnson et al. 2005). Asterisks note hornblende dissolution experiments that were stirred. The light gray box represents the field for DIR experiments that encompasses data from the end of the experiments (~1% to 10% dissolution). Data in panel *a* are most directly comparable across all experimental conditions because they reflect the proportion of Fe that is dissolved. Comparison of data in panel *b* across the experiments is more difficult because of variations in the experiments in terms of the mass of initial materials and volume of solutions; data from the DIR experiments are normalized to a total system size of 50 mM Fe. Also shown in panel *b* are the fields for riverine Fe and pore water Fe from modern marine sediments produced by DIR from **Figure 1**.

is probably responsible for producing the largest inventories of low-δ^{56}Fe Fe^{2+}_{aq}. This interpretation is supported by experimental studies of DIR, and in **Figure 2** we compare these results with experiments that studied abiologic dissolution of minerals. Hornblende leaching experiments in the presence of various organic ligands produced small quantities of aqueous Fe (~0.01% of the hornblende mass) that had δ^{56}Fe values up to 1.0‰ lower than the initial starting material (Brantley et al. 2001, 2004), in which the largest fractionations were observed in experiments that were actively agitated (**Figure 2*a***). Partial dissolution of goethite by oxalate, performed in light and in darkness, produced a wide range of δ^{56}Fe values that increased with increasing percent dissolution (**Figure 2*a***) (Wiederhold et al. 2006); these experiments were conducted under conditions of constant agitation, and the lowest δ^{56}Fe values for

Fe^{2+}_{aq} reflected approximately an order of magnitude greater dissolution than that obtained in Brantley and colleagues' (2004) hornblende leaching experiments that were agitated.

In contrast to the results for the abiologic partial dissolution of oxide/hydroxide or silicates, DIR experiments produced much larger proportions of Fe^{2+}_{aq} that had low-δ^{56}Fe values (**Figure 2*a***) (Beard et al. 1999, 2003a; Crosby et al. 2005, 2007; Johnson et al. 2005), and this contrast is particularly striking given that the DIR experiments were not actively stirred or agitated. The DIR experiments illustrated in **Figure 2** include those that compared members of the *Geobacteraceae* and *Shewanella* species, and the results for both bacteria were the same. Instead, the major differences in the δ^{56}Fe values for Fe^{2+}_{aq} seem to lie in the nature of the ferric oxide/hydroxide substrate (**Figure 2**). At ~1% to 10% total reduction, the δ^{56}Fe values for Fe^{2+}_{aq} range between 1.0‰ and 1.8‰ lower than the initial oxide/hydroxide for experiments that used goethite or hematite, and greater quantities of Fe^{2+}_{aq} were produced that had lower δ^{56}Fe values when ferrihydrite was used as the ferric Fe substrate. When cast in terms of concentrations for Fe^{2+}_{aq} (**Figure 2*b***), the experimental results lie within the range measured in natural fluids that are ascribed to DIR.

Our discussion above leads to the conclusion that the engine that produces the most significant quantities of low-δ^{56}Fe Fe^{2+}_{aq} in natural diagenetic environments is DIR, and this engine is fueled by a continual supply of organic carbon and reactive Fe^{3+} in many marine environments. We can write the overall reaction for DIR as

$$4Fe(OH)_3 + CH_2O + 8H^+ \rightarrow 4Fe^{2+}_{aq} + CO_2 + 11H_2O, \quad (4)$$

where, in marine environments, organic carbon (CH_2O) is supplied by primary photosynthetic productivity, and $Fe(OH)_3$ (ferrihydrite) is supplied by detrital riverine components or atmospheric dust delivery (e.g., Canfield et al. 2005); in most environments in which DIR is active, $Fe(OH)_3$ is the limiting component, and DIR may be inhibited in environments in which BSR rates are high. Nevertheless, we stress that DIR in marine sediments is a dynamic process, in which a continual supply of $Fe(OH)_3$ and organic carbon supports a continual state of partial reduction of Fe^{3+} oxide/hydroxide by DIR, producing mobile Fe^{2+}_{aq} that may be lost to the oceans at large or may react with sulfide produced by BSR (e.g., Severmann et al. 2006).

The Mechanisms of Isotopic Fractionation During Microbial Iron Reduction

Recent experimental work has provided important breakthroughs in our understanding of the mechanisms that produce Fe isotope fractionation during microbial DIR. Based on the observation that *Shewanella* species may solubilize Fe^{3+} prior to reduction, Beard et al. (2003a) and Johnson et al. (2004) proposed that the low-δ^{56}Fe values for Fe^{2+}_{aq} produced during DIR may reflect isotopic fractionation between Fe^{2+}_{aq} and a ligand-bound Fe^{3+} reservoir that had high-δ^{56}Fe values. This proposal was not based on direct measurement of the high-δ^{56}Fe component that was required by isotopic mass balance, and this component was not directly measured in the subsequent studies of Beard et al. (1999), Icopini et al. (2004), and Johnson et al. (2005).

Crosby and colleagues' (2005, 2007) experiments, however, showed that the ligand-bound Fe^{3+} model was incorrect and instead demonstrated, through direct analysis of the high-δ^{56}Fe Fe^{3+} component, that the δ^{56}Fe values for Fe^{2+}_{aq} were largely controlled by equilibrium isotope exchange with a reactive surface layer on the ferric oxide/hydroxide surface (defined as Fe^{3+}_{reac}). Crosby et al. (2007) showed that the δ^{56}Fe values for Fe^{2+}_{aq} may be described to a first approximation by the equation

$$\delta^{56}Fe_{Fe^{2+}_{aq}} = \Delta^{56}Fe_{Fe^{2+}_{aq}-Fe^{3+}_{reac}} X_{Fe^{3+}_{reac}}, \quad (5)$$

where $\Delta^{56}Fe_{Fe^{2+}_{aq}-Fe^{3+}_{reac}}$ is the Fe^{2+}_{aq}–ferric oxide/hydroxide fractionation factor (−3.0‰) (Johnson et al. 2002, Skulan et al. 2002, Welch et al. 2003), and $X_{Fe^{3+}_{reac}}$ is the mole fraction of Fe^{3+}_{reac} in the pool of Fe that is open to isotopic exchange, which is approximated by the sum of Fe^{2+}_{aq} and Fe^{3+}_{reac}.

Equation 5 describes well the relations between Fe^{2+}_{aq} and Fe^{3+}_{reac} for hematite substrates (**Figure 3*a***) because the isotopic effects of sorbed Fe are <0.05‰ (**Figure 3*b***), reflecting the small proportion of sorbed Fe and the fact that the Fe^{2+}_{aq}-Fe^{2+}_{sorb} fractionation is only −0.3‰ for hematite. The isotopic effects of sorption are significant during the initial stages of DIR when goethite is the substrate because the proportion of sorbed Fe is relatively large during the initial stages of reduction, increasing the influence of the Fe^{2+}_{aq}-Fe^{2+}_{sorb} fractionation factor for goethite (−0.9‰). Importantly, the net effect of sorption is never equal to the Fe^{2+}_{aq}-Fe^{2+}_{sorb} fractionation factor because mass-balance constraints among Fe^{2+}_{aq}, Fe^{2+}_{sorb}, and Fe^{3+}_{reac} also control the absolute δ^{56}Fe values (Crosby et al. 2007). In the case of goethite, the proportion of sorbed Fe decreases in the reactive Fe pool with increasing reduction, decreasing the net effect of sorption to only a few tenths per mil. Although large isotopic effects due to sorption have been proposed (Icopini et al. 2004, Teutsch et al. 2005), these studies did not account for isotopic mass balance among all the species open to isotopic exchange. In general, the net effects of sorption are small unless the $Fe^{2+}_{aq}/Fe^{2+}_{sorb}$ ratio is very low.

Crosby and colleagues' (2005, 2007) studies demonstrate that the Fe isotope fractionations produced by DIR are fundamentally equilibrium isotope fractionations, in which the role of bacteria appears to lie in catalyzing coupled atom (isotopic) and electron exchange. Could isotopic exchange between Fe^{2+}_{aq} and Fe^{3+}_{reac} be induced in completely abiologic systems? Enriched isotope tracer experiments have demonstrated isotopic exchange between Fe^{2+}_{aq} and ferric oxide/hydroxides (e.g., Williams & Scherer 2004, Pedersen et al. 2005), although these experiments were designed to measure neither shifts in Fe isotope ratios nor the size of the Fe inventories involved in isotopic exchange. Preliminary results indicate that isotopic exchange between Fe^{2+}_{aq} and hematite can be induced in an entirely abiologic system, but not to the extent that exchange occurs during microbial DIR, particularly in complex solutions (**Figure 3**). Crosby (2005) investigated Fe isotope fractionations in abiologic mixtures of Fe^{2+}_{aq} and hematite in proportions that matched those attained at the end of DIR experiments using the same substrate (Crosby et al. 2005). Despite active stirring, a significantly smaller proportion of Fe^{3+}_{reac} was produced in the abiologic experiments as compared with the DIR experiments, which were not stirred,

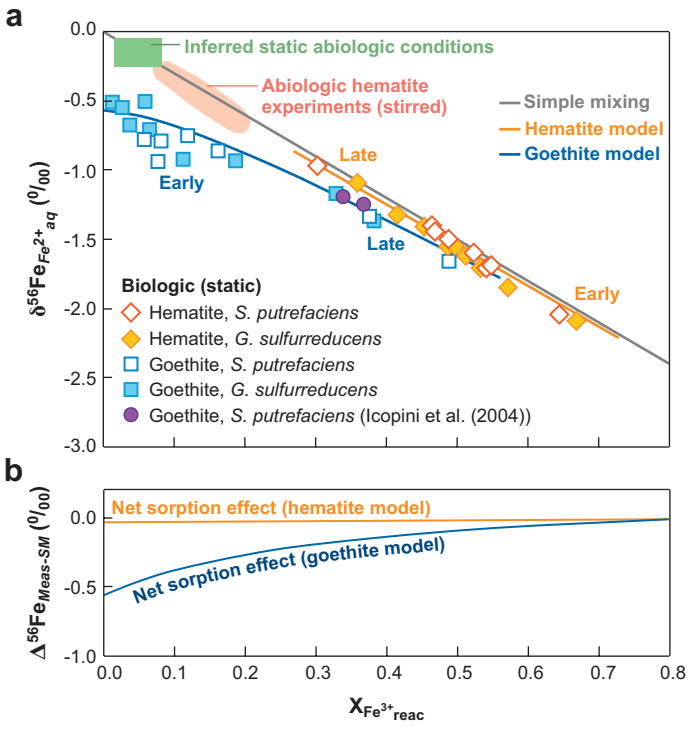

Figure 3

Iron isotope variations produced by dissimilatory iron reduction (DIR) of goethite and hematite and comparison to abiologic Fe^{2+}_{aq}-hematite interactions as a function of the mole fraction of Fe^{3+} in the reactive Fe pool ($X_{Fe^{3+}_{reac}}$). (*a*) The negative correlation between $\delta^{56}Fe$ values for Fe^{2+}_{aq} and $X_{Fe^{3+}_{reac}}$ can be described by a simple two-component mixing equation, and the data obtained for hematite closely follow this, reflecting the insignificant effect of sorption for experiments involving hematite (Crosby et al. 2007). The effects of sorption are significant during the early stages of DIR of goethite but decrease during continued reduction. (*b*) The net effects of sorption, defined as the $\delta^{56}Fe$ value measured for Fe^{2+}_{aq} relative to that predicted by the two-component mixing line, at a given $X_{Fe^{3+}_{reac}}$. In contrast to the biologic experiments involving hematite and dissolved silica, abiologic Fe^{2+}_{aq}-hematite interactions produce little reactive Fe^{3+}, which in turn produce only slightly negative $\delta^{56}Fe$ values for Fe^{2+}_{aq}. It is important to note that the abiologic experiments were actively stirred, whereas the biologic experiments were not, and the inferred conditions for static abiologic Fe^{2+}_{aq}-hematite interactions in the presence of dissolved silica are shown by the box in the upper left corner. Experimental data from Icopini et al. 2004; Crosby et al. 2005, 2007; and Kennedy et al. 2006.

producing a commensurate smaller shift in $\delta^{56}Fe$ values for Fe^{2+}_{aq} (**Figure 3**). In addition, abiologic experiments run with dissolved silica, intended to mimic the conditions of the Archean oceans, further inhibited Fe isotope exchange between Fe^{2+}_{aq} and hematite, suggesting that the presence of surface-sorbed species other than Fe may inhibit isotopic exchange in the absence of biology (Kennedy et al. 2006). These preliminary abiologic experiments suggest that under static conditions and in complex aqueous solutions, isotopic exchange between Fe^{2+}_{aq} and hematite will be suppressed

(**Figure 3**). It is not yet known if goethite and ferrihydrite behave similarly. Importantly, silica does not inhibit Fe reduction rates for DIR that utilizes ferrihydrite as the terminal electron acceptor (Kukkadapu et al. 2004; E. Roden, unpublished data).

The evidence at hand therefore indicates that abiological Fe^{2+}_{aq}–hematite interactions are unlikely to masquerade as a DIR fingerprint, although further experimental investigations are required to completely understand the process in systems that match natural conditions in terms of fluid compositions and Fe^{3+} substrate. The results from natural and experimental systems indicate that microbial DIR is far more efficient than abiologic exchange at producing a reactive Fe^{3+} layer, which in turn produces larger decreases in $\delta^{56}Fe$ values for Fe^{2+}_{aq} in biological systems relative to abiological analogs. We speculate that this contrast arises because iron-reducing bacteria actively pump electrons to the oxide surface (e.g., DiChristina et al. 2005), which catalyzes isotopic exchange to an extent not attained in equivalent abiologic systems. Atomic force microscopy has shown that outer membrane cytochromes in *Shewanella oneidensis* develop significant bonding energies at the interface with goethite (Lower et al. 2001, 2007). Recent studies have indicated that both *Geobacter* and *Shewanella* species are also capable of synthesizing specialized electrically conductive pili (nanowires), which may provide a means for transporting electrons to insoluble Fe oxides (Reguera et al. 2005, Gorby et al. 2007), promoting isotopic exchange. We speculate that both outer membrane–associated cytochromes and nanowires may transport electrons even in the presence of competing sorbed species such as silica, which in turn should allow isotopic exchange to still occur between Fe^{2+}_{aq} and ferric oxides during microbial Fe^{3+} reduction where such exchange would otherwise not occur in equivalent abiologic systems. Finally, we note that if the isotopic biosignature for bacterial iron reduction is independent of species or the nature of the electron donor, as seems possible from Crosby and colleagues' (2005, 2007) results, Fe isotopes will be a powerful means for tracing biogeochemical cycling in early Earth because it is unclear which species may have driven Fe reduction in the Archean. Iron reduction is phylogenetically diverse, found throughout the Bacteria and Archaea, including hyperthermophiles, sulfate reducers, nitrate reducers, and methanogens, involving a wide variety of electron donors (e.g., Lovley et al. 2004).

IRON-SULFUR INTERACTIONS DURING MARINE DIAGENESIS

Dissimilatory metal and sulfate reduction are the dominant pathways of organic carbon oxidation in many continental margin sediments, and the ultimate end product of coupled Fe-S cycling in marine sediments is pyrite. In the presence of sulfide, reactive Fe^{2+} and/or Fe^{3+} combines to form aqueous FeS species, which in turn form nanoparticulate FeS (mackinawite), which is an important precursor phase to pyrite formation (e.g., Rickard & Luther 1997, Benning et al. 2000, Schoonen 2004). Matthews et al. (2004) were the first to propose that sedimentary pyrite may record the $\delta^{56}Fe$ values of Fe^{2+}_{aq} produced by DIR, and below we explore the relations among reactive iron oxides, Fe^{2+}_{aq}, FeS, and pyrite in marine sediments, and the

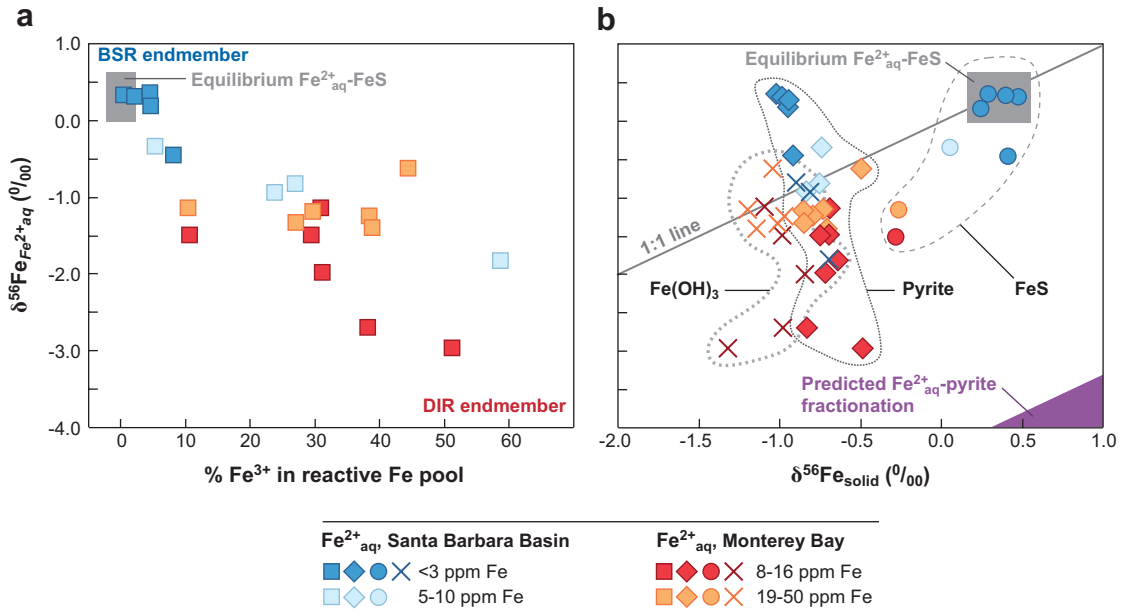

Figure 4

Variations in the Fe isotope compositions of pore water Fe^{2+}_{aq} relative to the oxidation state of reactive Fe and Fe isotope compositions of solid reactive Fe components from modern marine sediments from the Santa Barbara Basin and Monterey Bay California margin (Severmann et al. 2006). Correlations between the $\delta^{56}Fe$ values for Fe^{2+}_{aq} and the percentage of Fe^{3+} in the reactive Fe pool (HCl-extractable Fe) are illustrated in panel *a*, and those relative to the $\delta^{56}Fe$ values for solid reactive Fe phases are illustrated in panel *b*, including $Fe(OH)_3$ (*crosses*), FeS (*circles*), and pyrite (*diamonds*). The $\delta^{56}Fe$ values for FeS were estimated from HCl extractions that contained >80% Fe^{2+}, whereas the $\delta^{56}Fe$ values for $Fe(OH)_3$ were estimated from extractions that contained <80% Fe^{2+}, using the mixing relations given in Severmann et al. (2006). The estimated equilibrium Fe^{2+}_{aq}-FeS fractionation (*gray box*) is from Butler et al. (2005). The field encompassing the predicted Fe^{2+}_{aq}-pyrite fractionation factor at 25°C uses calculations from Schauble et al. (2001), Anbar et al. (2005), and Polyakov et al. (2007). BSR, bacterial sulfate reduction; DIR, dissimilatory iron reduction.

possibility that sedimentary pyrite may represent a permanent record of both BSR and DIR.

Correlations between the proportion of Fe^{3+} that composes the reactive pool of Fe (pore fluid + HCl-extractable Fe) and the $\delta^{56}Fe$ values for Fe^{2+}_{aq} in modern marine sediments from the California margin (**Figure 4*a***) led Severmann et al. (2006) to conclude that the Fe isotope compositions of Fe^{2+}_{aq} reflected mixtures between low-$\delta^{56}Fe$ Fe^{2+}_{aq} produced by DIR (associated with a high percentage of Fe^{3+} in the reactive Fe pool) and high-$\delta^{56}Fe$ Fe^{2+}_{aq} controlled by isotopic exchange with FeS (low percentage Fe^{3+} in the reactive Fe pool). The source of sulfide in the sediments ultimately reflects BSR, so we define a BSR end member for samples that contain no Fe^{3+} in the reactive Fe pool (**Figure 4*a***). The inferred $\delta^{56}Fe$ values of

$\sim$+0.5‰ for FeS in the HCl-extractable components (zero reactive Fe^{3+}) approximately equal those for Fe^{2+}_{aq} in the same samples, consistent with the near-zero or slightly positive Fe^{2+}_{aq}-FeS fractionation factor inferred by Butler et al. (2005) to approach equilibrium conditions. Pore water Fe^{2+} that has lower δ^{56}Fe values is out of isotopic equilibrium with FeS and instead is controlled by the production of low-δ^{56}Fe Fe^{2+}_{aq} by DIR, suggesting that the rate of Fe^{2+}_{aq} production by DIR exceeds that of isotopic exchange between Fe^{2+}_{aq} and FeS.

Exploring the relations among Fe^{2+}_{aq}, FeS, pyrite, and reactive Fe^{3+} in Severmann and colleagues' (2006) study in more detail, we see that FeS has δ^{56}Fe values distinct from those of pyrite in the same samples and that pyrite is far from isotopic equilibrium with Fe^{2+}_{aq} relative to the predicted Fe^{2+}_{aq}-pyrite fractionation factor (**Figure 4*b***). Although FeS is an important precursor to pyrite formation, pyrite did not inherit the Fe isotope compositions of FeS in the California margin sediments because FeS may exchange Fe isotopes with aqueous Fe^{2+} over timescales of days (Butler et al. 2005), suggesting that Fe^{2+}_{aq}-FeS equilibrium is more likely than Fe^{2+}_{aq}-pyrite equilibrium in sediments that are undergoing advective transport of porewater Fe^{2+}_{aq}. This is demonstrated by the fact that in no cases is pyrite in Fe isotope equilibrium with Fe^{2+}_{aq} based on predicted fractionation factors (**Figure 4**). Instead, we propose that the negative δ^{56}Fe values for pyrite reflect Fe^{2+}_{aq} that was generated by DIR and encountered sulfide that was generated by BSR.

Surprisingly, the estimated δ^{56}Fe values for the $Fe(OH)_3$ component in the HCl-extractable Fe substantially overlap with the δ^{56}Fe values measured for pyrite in the sediments (**Figure 4*b***). At first it may seem counterintuitive that Fe^{3+} may have the same δ^{56}Fe values as pyrite, but the negative δ^{56}Fe values inferred for $Fe(OH)_3$ are interpreted to reflect the rapid and complete oxidation of low-δ^{56}Fe Fe^{2+}_{aq} as reduced pore waters encountered oxidizing waters (Severmann et al. 2006). The low-δ^{56}Fe ferric oxide/hydroxides in diagenetic systems therefore provide an indirect proxy for DIR (Johnson & Beard 2006), consistent with Canfield and colleagues' (1993b) proposal that Fe undergoes redox cycling many times before ultimate burial. Isotopic mass balance for the sediments is provided by FeS, which has relatively high-δ^{56}Fe values (Severmann et al. 2006).

We conclude that the δ^{56}Fe values of sedimentary pyrite reflect a permanent repository of several Fe sources, including (*a*) detrital oxides that have reacted with sulfide (δ^{56}Fe = 0‰) (Beard et al. 2003b), (*b*) FeS precursors (δ^{56}Fe $\sim$ 0 to +0.5‰) (**Figure 4**), (*c*) the sulfidation of low-δ^{56}Fe ferric oxide/hydroxides that formed from DIR-produced Fe^{2+}_{aq}, and (*d*) the direct reaction of sulfide and low-δ^{56}Fe Fe^{2+}_{aq} that was produced by DIR. DIR is therefore important in two of these four Fe pathways. The Fe isotope compositions of pyrite cannot be explained by equilibrium Fe^{2+}_{aq}-pyrite exchange, which should produce pyrite that has positive δ^{56}Fe values. In diagenetic systems in which the proportion of low-δ^{56}Fe Fe^{2+}_{aq} or ferric oxide/hydroxide is small relative to other pools of reactive Fe, we expect sedimentary pyrite to have only modestly negative δ^{56}Fe values, and perhaps modestly positive values. Such cases are expected in which oxidation of organic carbon occurs largely by BSR rather than DIR. If, however, DIR activity exceeds that of BSR in terms of organic carbon oxidation, as would occur in environments where delivery of ferric oxides/hydroxides is high,

we expect the DIR contribution to the Fe isotope composition of pyrite to be much higher, shifting the δ^{56}Fe values of pyrite to more negative compositions. These contrasts in δ^{56}Fe values for BSR- or DIR-dominated compositions have been found in organic-rich shales that formed just before the Cenomanian-Turonian oceanic anoxic event (Jenkyns et al. 2007).

ANCIENT IRON REDOX CYCLING: PRECAMBRIAN SHALES, SULFIDES, AND BANDED IRON FORMATIONS

The largest inventories of Fe that are isotopically variable are recorded in Precambrian rocks that have undergone diagenesis, including shales that have high-Fe, -C, or -S contents, sedimentary pyrite, and banded iron formations (BIFs). The temporal variation in δ^{56}Fe values for Archean and Proterozoic sedimentary rocks suggests a marked increase in the abundance of Fe that had low-δ^{56}Fe values in the surface environments of Earth between ~3.1 and ~2.4 Ga (**Figure 5**). Proterozoic-age sedimentary pyrite generally has near-zero or slightly positive δ^{56}Fe values, whereas 2.7 to 2.5 Ga–age pyrite has significantly negative δ^{56}Fe values. Rouxel et al. (2005) interpreted the temporal changes in the Fe isotope compositions of sedimentary pyrite to be a direct proxy of ancient seawater during the commonly proposed rise in atmospheric O_2 contents in the early Proterozoic (e.g., Holland 1984), which in turn requires that the isotopic compositions remained unchanged by biogeochemical cycling during early diagenesis. The temporal changes in Fe isotope compositions for sedimentary pyrite are also seen in the Fe isotope record for shales (**Figure 5**). Although relatively few Fe-, C-, or S-rich Proterozoic shales have been analyzed for Fe isotope compositions, these appear to have significantly higher δ^{56}Fe values than late Archean shales of similar bulk chemical composition (Yamaguchi et al. 2005, Rouxel et al. 2006), and they overlap the range in δ^{56}Fe values of sedimentary pyrite of the same age. An important observation, however, is that near-zero and moderately negative δ^{56}Fe values are measured in shales of ~3.3 to ~2.9 Ga. In addition, data from early Archean BIFs (3.7 to 3.8 Ga) indicate that positive or near-zero δ^{56}Fe values may characterize sedimentary rocks during this time. We explore the implications of these temporal changes in the subsections that follow.

Figure 5

Temporal variation in δ^{56}Fe values for minerals (*a*) and bulk shales (*b*) that are C-, S-, or Fe-rich, reflecting the range in Fe isotope compositions produced during diagenetic reactions in the Archean and Proterozoic. A total of 487 samples is represented, including 114 pyrites (Rouxel et al. 2005, Archer & Vance 2006), 81 bulk shales (Yamaguchi et al. 2005, Rouxel et al. 2006), 39 samples of the 1.8 Ga Biwabik banded iron formation (BIF) (Rouxel et al. 2005, Frost et al. 2006, Hyslop et al. 2008), 162 samples from the 2.5 Ga Hamersley-Transvaal BIFs (Johnson et al. 2003, 2008), and 91 samples from early Archean BIFs (Dauphas et al. 2004, 2007; Whitehouse & Fedo 2007; Herrick 2007). The horizontal gray bands mark the range in δ^{56}Fe values for additional data for low-C and low-S clastic sedimentary rocks of modern to Archean age (114 samples) (Beard et al. 2003b, Yamaguchi et al. 2005).

Banded Iron Formations

Unusual periods of high iron deposition in low-energy marine environments are recorded in BIFs, which largely occur in the Archean and early Proterozoic (e.g., Klein 2005). The large inventory of Fe^{3+}-bearing oxides (magnetite, hematite) requires an oxidant during BIF genesis, given that all proposed iron sources (riverine, marine hydrothermal) were Fe^{2+}. The nature and quantity of this oxidant, however, are not

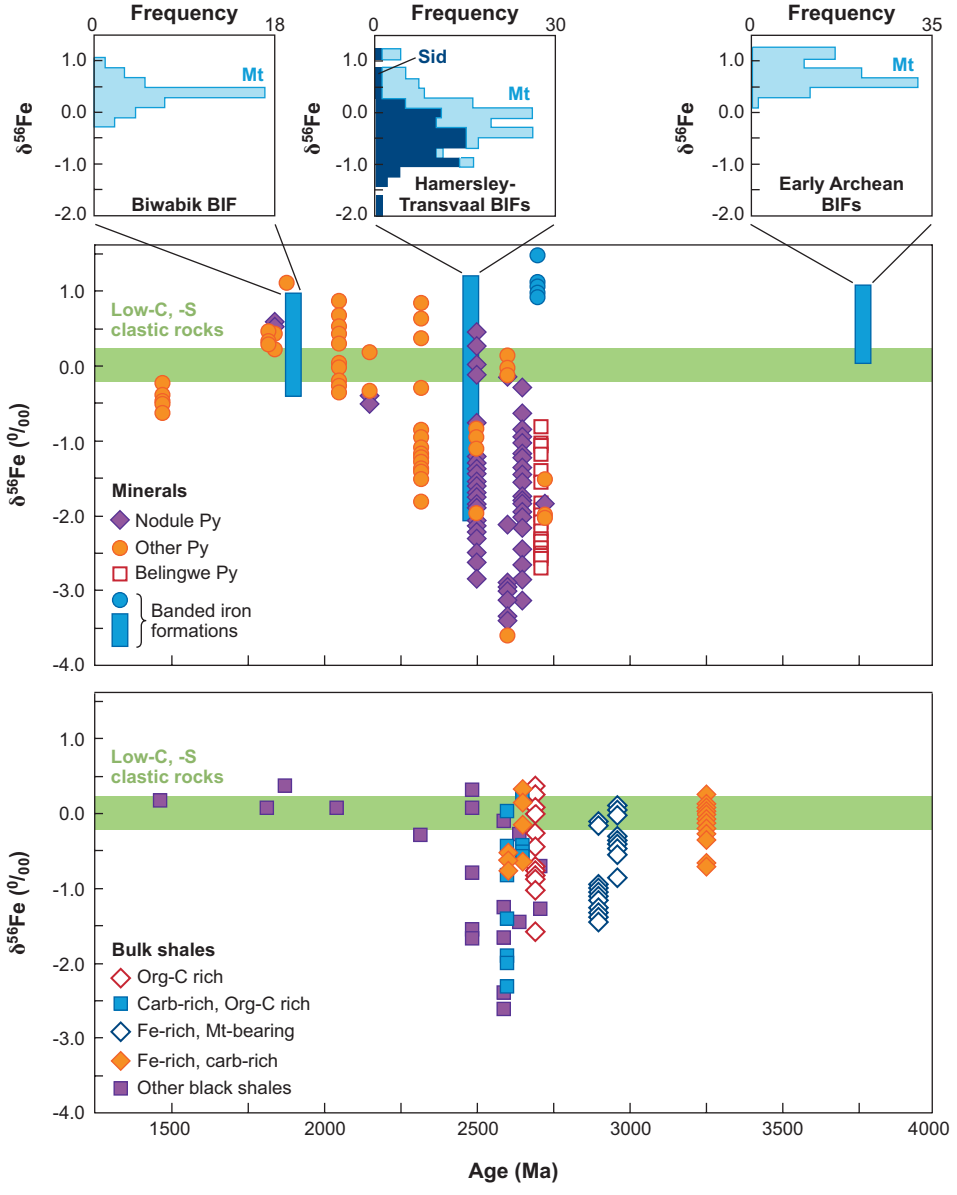

clear and may have included atmospheric O_2 (Cloud 1968), anaerobic photosynthetic Fe^{2+}-oxidizing bacteria (Widdel et al. 1993), or UV photo-oxidation (Braterman & Cairnssmith 1987), although recent experimental work apparently rules out UV photo-oxidation as a viable mechanism in natural seawater compositions (Konhauser et al. 2007). Iron isotope data are available for BIFs from three time periods in the Precambrian: ~3.7–3.8 Ga, ~2.5–2.7 Ga, and ~1.8–1.9 Ga (**Figure 5**). The temporal variations in δ^{56}Fe values for BIFs from these time periods are similar to those observed in bulk shales or sedimentary pyrite, in which early Archean BIFs have near-zero to positive δ^{56}Fe values; the 2.5 to 2.7 Ga BIFs have a wide range in δ^{56}Fe values, extending to very negative values; and the ~1.9 Ga BIFs have near-zero to positive δ^{56}Fe values, similar to those measured for the early Archean BIFs (**Figure 5**). Most of the Fe isotope data from these BIFs were obtained on magnetite or magnetite-rich samples, although pyrite was also analyzed from the 3.7–3.8 Ga Isua BIFs, which have positive δ^{56}Fe values that overlap with those measured for magnetite in the Isua BIFs (Whitehouse & Fedo 2007). In addition, siderite has been extensively sampled in the 2.5 Ga BIFs, which tend to have lower δ^{56}Fe values than magnetite in the same samples (Johnson et al. 2008).

The most detailed studies have focused on the 2.5 Ga BIFs of the Hamersley Group (Australia) and Transvaal Supergroup (South Africa), which represent the largest BIF deposits on Earth and contain sections that have not been significantly metamorphosed (Johnson et al. 2003, 2008; Klein 2005). Although the δ^{56}Fe values for magnetite from the Hamersley-Transvaal BIFs range from −1.0‰ to +1.2‰, the average δ^{56}Fe value is 0.0‰, suggesting an overall isotopic mass balance relative to the inferred δ^{56}Fe values for hydrothermal Fe and ferric Fe oxide/hydroxide inputs, which are estimated to have had near-zero δ^{56}Fe values (Johnson et al. 2008). The peak in δ^{56}Fe values of magnetite at 0‰ (**Figure 5**) is thought to be inherited from ferric oxide/hydroxide precursors that formed through complete oxidation of Fe^{2+}_{aq}, followed by conversion to magnetite through interaction with Fe^{2+}_{aq} that was sourced to hydrothermal fluids, or reduction by iron-reducing bacteria (Johnson et al. 2008). Magnetite that has positive δ^{56}Fe values is interpreted to reflect inheritance from ferric oxide/hydroxide precursors produced by the incomplete oxidation of hydrothermal Fe^{2+}_{aq}, whereas magnetite that has negative δ^{56}Fe values is interpreted to have incorporated low-δ^{56}Fe Fe^{2+}_{aq} formed by DIR (Johnson et al. 2008).

The Fe isotope compositions of siderite from the Hamersley-Transvaal BIFs reflect Fe pathways that are distinct from those that formed magnetite (Johnson et al. 2008). The peak in δ^{56}Fe values at ~−0.5‰ for siderite (**Figure 5**) is interpreted to reflect a major control by seawater Fe, in which the estimated near-zero δ^{56}Fe values for late Archean seawater would produce siderite that had δ^{56}Fe values of ~−0.5‰ (Johnson et al. 2008), using Wiesli and colleagues' (2004) experimentally determined Fe^{2+}_{aq}-siderite fractionation factor. Siderite that has δ^{56}Fe values that deviate from this average may reflect inheritance from precursor ferric oxide/hydroxides (δ^{56}Fe ~ 0‰), followed by complete reduction by iron-reducing bacteria, or the effects of Ca substitution on the Fe^{2+}_{aq}-carbonate fractionation factor (δ^{56}Fe < −0.5‰) (Johnson et al. 2008).

An important issue in interpreting the Fe isotope record of Archean and Proterozoic sedimentary rocks is if these compositions directly reflect those of ancient seawater, as advocated by Rouxel et al. (2005) or if they reflect biogeochemical cycling during early sediment diagenesis, as suggested by Yamaguchi et al. (2005). The large range in δ^{56}Fe values for magnetite and siderite of up to 2‰ from the BIFs of the Dales Gorge member of the Brockman Iron Formation, Hamersley Group over time intervals on the order of 10^3 years seems best explained by diagenesis, not by rapid changes in the δ^{56}Fe values of seawater (Johnson et al. 2008). Rapid changes in seawater δ^{56}Fe values require relatively low residence times (<100 years), although even in modern marine hydrogenous and hydrothermal sediments there appears to be no isotopic variation over timescales of $\sim 10^4$ years (Johnson et al. 2008). It is generally accepted that the Fe residence times were longer in the Archean, prior to oxygenation of the deep oceans, which would make it even more difficult to rapidly change seawater δ^{56}Fe values. Based on the range in estimated Fe contents of Archean seawater of 2 to 50 ppm (Ewers 1983, Sumner 1997, Canfield 2005), the Fe residence time in the Archean may have ranged from 10,600 to 236,000 years; even if a relatively short time of 10 kyr is used, the temporal changes in δ^{56}Fe values for the Dales Gorge BIFs cannot be produced (Johnson et al. 2008), providing strong support that their Fe isotope compositions cannot directly reflect those of seawater. Similar conclusions may be made from the Fe isotope data obtained on sedimentary pyrite from the 2.7 Ga Belingwe sedimentary basin (Zimbabwe), in which Archer & Vance (2006) noted that δ^{56}Fe values vary by 2‰ over a 10-cm interval. When viewed in the light of temporal Fe isotope variations for modern marine sediments, as well as in consideration of the likely Fe residence times in the Archean oceans, the wide range in δ^{56}Fe values for sedimentary pyrite and shales between 3.0 and 2.2 Ga (**Figure 5**) seems unlikely to us to reflect large fluctuations in the Fe isotope compositions of seawater.

Issues of Isotopic Mass Balance in the Archean

That bulk sedimentary rocks of Archean age have δ^{56}Fe values that deviate from zero suggests that the inventory of Fe that was actively cycled, and hence subject to Fe isotope fractionation, was significantly larger in the past than it is today. The inventory of Fe that has nonzero δ^{56}Fe values in modern surface environments is extremely small. We note above that the dissolved riverine load is relatively small, as is the total dissolved Fe inventory in the oceans, which is inferred to have generally negative δ^{56}Fe values (e.g., Levasseur et al. 2004). The inventory of isotopically variable Fe contained in diagenetic pore fluids and reactive oxide/hydroxides and sulfides from Cenozoic marine sediments is also small (Bergquist & Boyle 2006, Severmann et al. 2006, Staubwasser et al. 2006), which is demonstrated by the fact that total digests of these sediments yield δ^{56}Fe values near zero. An important exception exists for bulk samples of black shales that were deposited immediately before the Cenomanian-Turonian oceanic anoxic event, which have δ^{56}Fe values as low as −1.7‰ (Jenkyns et al. 2007).

If the large number of nonzero δ^{56}Fe values measured for late Archean and early Proterozoic rocks (**Figure 5**) reflects a significant inventory of isotopically variable Fe that does not exist today, how large could this inventory have been? Many Archean shales have Fe/Ti ratios that are significantly higher than the igneous rock average (Kump & Holland 1992), suggesting that such rocks may indeed reflect relatively rich repositories of Fe that had been mobilized. Such Fe enrichment, however, is generally not recorded in younger sediments, indicating that high Fe/Ti ratios did not characterize major portions of the surface environment in the Archean, assuming that the younger sediments would have contained some component of recycled older sediments (Kump & Holland 1992). This in turn suggests that the inventory of Fe that had nonzero δ^{56}Fe values in the Archean may have been restricted to specific surface environments. The total Fe inventory in modern marine sediments is $\sim 1.2 \times 10^{20}$ mol, and this is equivalent to the total Fe inventory contained in the upper 150 m of the continental crust today (Lecuyer & Ricard 1999). If, for example, 10% of the marine sediment inventory in the Archean had a δ^{56}Fe value of $-1.0‰$, this may be balanced by the Fe contained in only 15 m of upper continental crust if this Fe had a δ^{56}Fe value of $+1.0‰$, assuming the relative sediment and crustal proportions of today. If Archean seawater had Fe contents between 2 and 50 ppm (see above), the total Fe inventory in the oceans would lie somewhere between 5.4×10^{16} and 1.2×10^{18} mol, which is small relative to the sediment and upper crustal Fe inventories. We conclude that although it seems clear that there were much larger inventories of nonzero δ^{56}Fe sedimentary rocks in the late Archean and early Proterozoic than there are today (probably by several orders of magnitude), the required isotopic mass balance for this inventory could be contained in a relatively small proportion of the continental crust. Full understanding of the mass-balance issues of isotopically variable Fe inventories in the Precambrian will probably require detailed basinwide studies of sedimentary pyrite and shales, which have yet to be completed. In this regard, it is noteworthy that the magnetite inventory in the 2.5 Ga Hamersley-Transvaal BIFs appears to be isotopically balanced about $\delta^{56}\text{Fe} = 0$, and the average δ^{56}Fe value for siderite can be controlled by the estimated Fe isotope composition of seawater, thus satisfying isotopic mass balance for the Fe-bearing BIF minerals (Johnson et al. 2008).

Isotopic Coupling of the Microbial C-S-Fe Systems

Sufficient C, S, and Fe isotope data for Archean and Proterozoic sedimentary rocks now exist to allow us an integrated first look into the C-S-Fe biogeochemical cycling that occurred in ancient Earth, which in turn provides important constraints on the evolution of life and the changing surface conditions of early Earth. It has long been recognized that the development of autotrophic fixation of CO_2, including photosynthesis, marked a critical milestone for the evolution of life, and below we argue that photosynthesis was the ultimate driving force in determining the ancient Fe isotope record. Multiple lines of evidence have been used to constrain when photosynthesis evolved, including morphological, phylogenetic, molecular biomarker, and C isotope data (e.g., Schopf 1993, Brocks et al. 1999, Xiong et al. 2000, Schidlowski

2001, Brasier et al. 2002, van Zullen et al. 2002, Rosing & Frei 2004, Kopp et al. 2005, Zerkle et al. 2005, Hayes & Waldbauer 2006, Olson 2006). Many workers have argued that the earliest photosynthesis was anoxygenic, and particular attention has been focused on anaerobic photosynthetic Fe^{2+} oxidation because of the likelihood that $Fe^{2+}{}_{aq}$ was the most important electron donor in the early Archean oceans (e.g., Widdel et al. 1993, Canfield 2005, Olson 2006), possibly reflecting ~90% of ocean primary productivity in the early Archean (Canfield et al. 2006). Investigators have used anaerobic photosynthetic Fe^{2+} oxidation to explain key components of the early Archean rock record such as BIFs (Widdel et al. 1993, Kappler et al. 2005) and stromatolites (Bosak et al. 2007). It is important to note that anaerobic photosynthetic Fe^{2+} oxidation produces organic carbon that may be used in heterotrophic respiration such as DIR and BSR, as well as providing a source of Fe^{3+} that is essential to DIR, as shown by the reaction

$$7H_2O + 4Fe^{2+} + CO_2 \rightarrow CH_2O + 4FeOOH + 8H^+. \quad (6)$$

The C isotope fractionations produced by anaerobic photosynthetic Fe^{2+} oxidation are generally the same as those of oxygenic photosynthesis (e.g., Zerkle et al. 2005), although there are exceptions (J. Brocks, personal communication, 2007), so $\delta^{13}C$ values alone cannot distinguish between various types of photosynthetic pathways. Moreover, the evidence at hand suggests that anaerobic photosynthetic Fe^{2+} oxidation produces similar Fe isotope fractionations as abiologic Fe^{2+} oxidation (Croal et al. 2004). Although C and Fe isotopes do not provide unique fingerprints for anaerobic photosynthetic Fe^{2+} oxidation, the moderately negative $\delta^{13}C$ values and positive $\delta^{56}Fe$ values in early Archean sedimentary rocks suggests that some type of photosynthesis was operating and that only a fraction of the marine $Fe^{2+}{}_{aq}$ inventory was oxidized to Fe^{3+}, indicating that the amount of oxidant was limited (e.g., Dauphas et al. 2004, Rosing & Frei 2004, Johnson & Beard 2006, Whitehouse & Fedo 2007).

Development of oxygenic photosynthesis marked a one to two orders of magnitude increase in ocean primary productivity relative to anaerobic photosynthesis (e.g., DesMarais 2000, Canfield et al. 2006, Rosing et al. 2006). Oxygenic photosynthesis is most simply written as

$$H_2O + CO_2 \rightarrow CH_2O + O_2. \quad (7)$$

In terms of C, S, and Fe cycling, invention of oxygenic photosynthesis was important because it provided much larger sources of organic carbon and, indirectly, Fe^{3+} through the oxidation of Fe^{2+} by O_2 than were likely to have been produced by anaerobic photosynthetic Fe^{2+} oxidation. This supports DIR, and oxidation of pyrite by O_2 produces $SO_4{}^{2-}$ in the oceans to support BSR. BSR is commonly represented as

$$SO_4{}^{2-} + CH_2O \rightarrow 2HCO_3{}^- + H_2S, \quad (8)$$

which therefore is analogous to DIR in its use of organic carbon (Canfield 2005). Support for coupling BSR to atmospheric O_2 contents comes from the S isotope record, in which a major increase in S isotope fractionations in sedimentary sulfides occurs at approximately ~2.4 Ga (e.g., Canfield 2001), coincident with the commonly

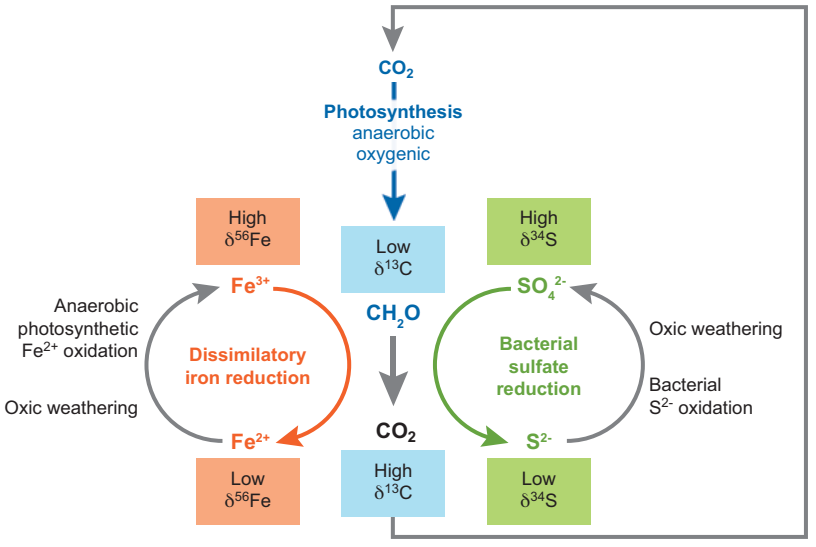

Figure 6

Illustration of the isotopic coupling that exists among C, S, and Fe in terms of bacterial cycling. Photosynthetic fixation of CO_2 as organic carbon (CH_2O) produces low $\delta^{13}C$ values of ~−25‰ to −35‰ (e.g., Hayes 2001). Oxidation of organic C by bacterial sulfate reduction (BSR) and dissimilatory iron reduction (DIR) is coupled to the reduction of SO_4^{2-} to S^{2-} and Fe^{3+} to Fe^{2+}, respectively, which produce decreases in the $\delta^{34}S$ and $\delta^{56}Fe$ values, respectively, relative to the initial substrate. There is little C isotope fractionation between CH_2O and the biomass (kerogen) produced by BSR or DIR (Londry & Des Marais 2003, Romanek et al. 2003), indicating that the $\delta^{13}C$ values of organic C-rich shales include a major component produced by photosynthesis, whereas S^{2-} and Fe^{2+} phases in shales tend to have low-$\delta^{34}S$ and -$\delta^{56}Fe$ values if BSR and DIR contributed these reduced components to the S and Fe inventory in the rocks, respectively.

proposed time of major increases in atmospheric O_2 (e.g., Holland 1984), although, as will be discussed below, the S isotope record supports the existence of BSR at some level earlier in Earth's history.

We bring the above discussion together into an integrated view of bacterial C-S-Fe cycling and their attendant isotopic fractionations in **Figure 6**. Photosynthetic fixation of CO_2 that is in equilibrium with carbonate in the oceans produces organic carbon that has negative $\delta^{13}C$ values, on the order of −25 to −35‰ (e.g., Hayes 2001), and this isotopic fingerprint is not significantly modified during incorporation into the biomass (kerogen) produced by BSR or DIR (Londry & Des Marais 2003, Romanek et al. 2003). Organic matter in sedimentary rocks may have lower $\delta^{13}C$ values, which has been interpreted to reflect biological cycling of CH_4, such as methanotrophy, which may provide an indirect record for oxygenic photosynthesis (e.g., Hayes 1983). Oxidation of Fe^{2+} may occur by anaerobic photosynthetic Fe^{2+} oxidation or other biologic and abiologic pathways, such as interaction with atmospheric O_2, and positive $\delta^{56}Fe$ values for Fe^{3+} species are produced for any of

these pathways if only a portion of the Fe^{2+} inventory is oxidized, or, if complete oxidation occurs, near-zero $\delta^{56}Fe$ values may be produced (e.g., Johnson & Beard 2006). DIR couples the reduction of Fe^{3+} to Fe^{2+} to oxidation of organic matter, producing negative $\delta^{56}Fe$ values for $Fe^{2+}{}_{aq}$, as discussed above. Photosynthesis (anaerobic or oxygenic) and DIR, therefore, form a C-Fe couple (e.g., Canfield 2005). An analogous couple for C and S occurs via BSR. Sulfate in the oceans generally reflects oxidative weathering of pyrite by free O_2, producing sulfate (e.g., Canfield 2001). BSR couples reduction of SO_4^{2-} to S^{2-} to oxidation of organic matter, producing negative $\delta^{34}S$ values for sulfide that is ultimately sequestered as sedimentary pyrite, which are balanced by positive $\delta^{34}S$ values in the remaining SO_4^{2-} reservoir; the most negative $\delta^{34}S$ values are produced if SO_4^{2-} exists in excess (e.g., Canfield 2001). If all three components of the bacterial C-S-Fe cycle occur in the same sedimentary basin (photosynthesis, BSR, and DIR), these cycles may be recorded in the isotopic compositions contained in the rock inventory. Such an example can be found in the C, S, and Fe isotope data on black shales of the Spring Valley and Jimmy members of the 2.7 Ga Manjeri Formation, Belingwe sedimentary basin, which have $\delta^{13}C$ values between −19 and −38‰ for organic carbon, and $\delta^{34}S$ and $\delta^{56}Fe$ values for sedimentary pyrite of −3 to −18‰ and −0.9 to −2.6‰, respectively, which has been interpreted to reflect coupled BSR and DIR via oxidation of organic carbon that was produced by photosynthesis (Grassineau et al. 2001, Archer & Vance 2006).

C, S, and Fe Isotope Variations in the Precambrian: Evidence for Coevolution of Multiple Microbial Metabolisms

Figure 7 explores the temporal record of $\delta^{13}C$, $\delta^{34}S$, $\Delta^{33}S$, and $\delta^{56}Fe$ values for sedimentary rocks of Proterozoic and Archean age within the context of the evolution of microbial metabolism. We divide our discussion into three parts based on the temporal Fe isotope record: (*a*) the period >3.1 Ga, (*b*) 3.1 to 2.4 Ga, and (*c*) <2.4 Ga. The moderately negative $\delta^{13}C$ values for organic carbon of early Archean age (>3.1 Ga) are generally accepted to reflect C fixation by photosynthesis (e.g., Des Marais 2001, Schidlowski 2001). Debate continues regarding the origin of low-$\delta^{13}C$ graphite in the 3.7–3.8 Ga high-grade rocks of the Isua supracrustal belt and at Akilia island in southwest Greenland, although the evidence seems less contentious at Isua (e.g., Rosing & Frei 2004). In addition, the C isotope record contains some evidence for methanogenesis in the early Archean (Ueno et al. 2006). Strong support for low atmospheric O_2 contents at >3.1 Ga comes from S isotope data for sedimentary sulfides, in which the restricted range in $\delta^{34}S$ values indicates generally low SO_4^{2-} contents in the oceans (e.g., Habicht et al. 2002), which in turn restricts BSR to low levels in the open ocean or occurrence in isolated environments (Canfield 2001). Although Shen et al. (2001) argued that BSR occurred as early as 3.5 Ga based on moderately negative $\delta^{34}S$ values in sulfides from the Dresser Formation (**Figure 7**), new studies suggest that the S isotope fractionations were produced by bacterial disproportionation of S° (Philippot et al. 2007). Significant, mass-independent fractionations among ^{32}S, ^{33}S, and ^{34}S (expressed as $\Delta^{33}S$ values) have figured prominently in discussions on

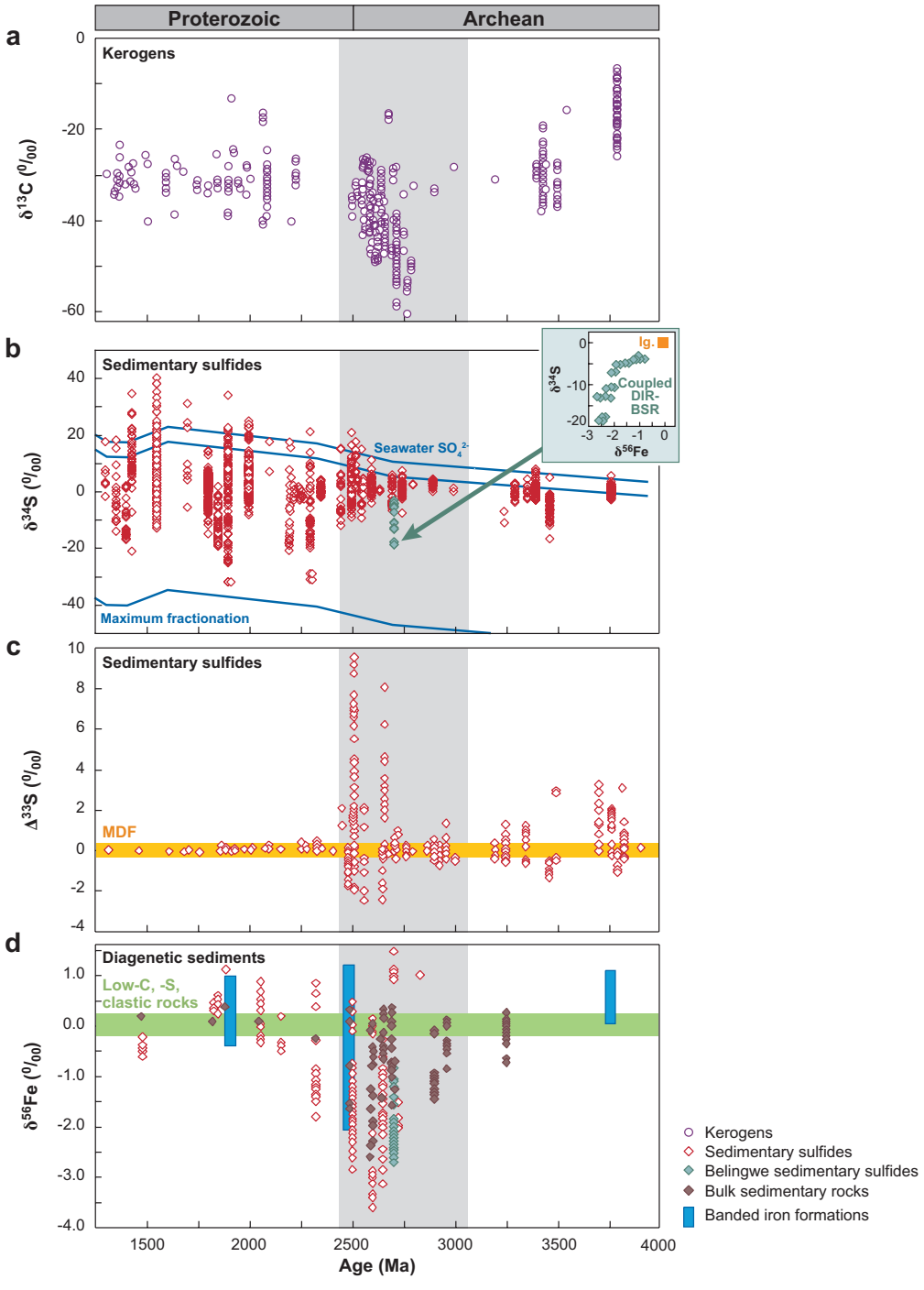

atmospheric O_2 contents, and the nonzero $\Delta^{33}S$ values for sulfides of Archean age have been taken as evidence for very low atmospheric O_2 contents during this time interval (e.g., Farquhar & Wing 2003).

The Fe isotope record for sedimentary rocks of >3.1 Ga age so far suggests relatively limited variation in $\delta^{56}Fe$ values (**Figure 7**), in which the positive $\delta^{56}Fe$ values at ~3.7–3.8 Ga are interpreted to reflect incomplete oxidation of the marine Fe^{2+}_{aq} inventory, as discussed above, and oxidation was most likely to have occurred through anaerobic photosynthetic Fe^{2+} oxidation in light of the evidence against UV photooxidation in natural seawater compositions (Konhauser et al. 2007). Canfield et al. (2006) suggest that primary ocean productivity in the early Archean was probably limited by the supply of Fe^{2+}_{aq}, and the fact that the Fe isotope data indicate incomplete oxidation suggests that productivity was not Fe limited, but instead may have been limited by other nutrients such as P (e.g., Bjerrum & Canfield 2002).

Major fluctuations occur in the temporal C, S, and Fe isotope record between ~3.1 and ~2.4 Ga (**Figure 7**). Most workers consider this interval to have had low atmospheric O_2 contents (e.g., Holland 1984), although several lines of evidence suggest that free O_2 may have been available, at least in local marine environments

Figure 7

Temporal variations in C, S, and Fe isotope compositions in Archean and Proterozoic rocks. A major transition in isotopic compositions between ~3.1 Ga and ~2.4 Ga is marked by a gray field. (*a*) Carbon isotope data from kerogens that record relatively low levels of thermal maturation. Although there is some debate regarding the primary nature of C isotope data from the 3.7–3.8 Ga Isua supracrustal belt, it is generally accepted that the moderately negative $\delta^{13}C$ values for organic carbon from ~3.5 Ga and younger samples reliably reflect primary compositions. Prior to ~2.8 Ga, the moderately negative $\delta^{13}C$ values probably reflect anaerobic photosynthesis, whereas the strong drop to more negative $\delta^{13}C$ values between ~2.8 and 2.6 Ga is interpreted to reflect methanotrophy or methanogenesis. (*b*) $\delta^{34}S$ values for sedimentary sulfides have relatively restricted ranges until ~2.4 Ga, at which time a major increase in atmospheric O_2 occurred, significantly increasing seawater SO_4^{2-} contents and hence the range in S isotope fractionations (e.g., Holland 1984). The inset in panel *b* shows $\delta^{34}S$ and $\delta^{56}Fe$ values from sulfides from the 2.7 Ga Belingwe sedimentary basin relative to igneous Fe and S ("Ig") that are interpreted to reflect coupled bacterial sulfate reduction (BSR) and dissimilatory iron reduction (DIR) (Archer & Vance 2006). The double blue line is the estimated range in $\delta^{34}S$ values for SO_4^{2-}, and the lower blue line marks the maximum fractionation with sulfide (Canfield 2001). (*c*) Mass-independent S isotope fractionations among ^{32}S, ^{33}S, and ^{34}S, expressed as $\Delta^{33}S$ values (Farquhar & Wing 2003), indicate relatively low atmospheric O_2 contents from ~3.8 to ~3.0 Ga, a possible increase from ~3.0 to ~2.7 Ga, low O_2 contents from ~2.7 to ~2.4 Ga, followed by a permanent increase at ~2.4 Ga. (*d*) Temporal changes in Fe isotope compositions from **Figure 5**. Collectively, the covariations in C, S, and Fe isotopes are interpreted to reflect an early period of photosynthesis (~3.8 to ~3.0 Ga) and an increase in DIR between ~3.0 Ga and ~2.5 Ga that reflects an increase in reactive Fe^{3+} and organic carbon from photosynthesis, combined with relatively low levels of BSR until ~2.4 Ga. The relatively high-$\delta^{56}Fe$ values in the Proterozoic reflect a decrease in DIR that accompanied an increase in BSR and transition to a sulfidic ocean at ~1.8 Ga. In addition to the publications noted above, data sources are from Shen et al. (2001), Eigenbrode & Freeman (2006), Hayes & Waldbauer (2006), Ohmoto et al. (2006), Ono et al. (2006), Farquhar et al. (2007), and references therein.

that have been characterized as oxygen oases (e.g., Kasting et al. 1992). The strong decrease in $\delta^{13}C$ values for organic carbon between ~2.8 and 2.7 Ga (**Figure 7**) has been proposed to reflect methanotrophy in the presence of free O_2 (Hayes 1983), which occurs via the reaction:

$$7CH_4 + 8O_2 \rightarrow 6CH_2O + CO_2 + 8H_2O. \quad (9)$$

Methane-related microbial cycling may produce very negative $\delta^{13}C$ values for organic carbon (e.g., Hayes et al. 1987, Summons et al. 1994, Hinrichs et al. 1999). Alternatively, anaerobic oxidation of methane may occur where sulfate is the terminal electron acceptor via the reaction:

$$CH_4 + SO_4^{2-} \rightarrow HCO_3^- + HS^- + H_2O \quad (10)$$

(e.g., Boetius et al. 2000, Orphan et al. 2002), and Hinrichs (2002) has proposed such a mechanism as an alternative explanation for the very low $\delta^{13}C$ values for organic carbon in late Archean sedimentary rocks. The negative $\delta^{34}S$ values in some sedimentary rocks of ~2.7 Ga age (**Figure 7**) may therefore suggest that, at least locally, seawater sulfate contents may have been high enough to support anaerobic oxidation of methane. Still, others have interpreted the strong decrease in $\delta^{13}C$ values at ~2.7 Ga to be unrelated to changes in microbial metabolism but instead to reflect changes in the rate of burial of organic carbon (e.g., Bjerrum & Canfield, 2004).

Additional lines of evidence suggest that free O_2 may have existed in the late Archean, and although this continues to be debated, resolution of these debates will affect our interpretation of the Fe isotope record. Evidence for oxygenic photosynthesis during this time interval comes from molecular biomarkers (e.g., Brocks et al. 2003), but the possibility of sample contamination by modern organic material remains a serious concern (Brocks et al. 2008). The small or zero $\Delta^{33}S$ values between ~2.9 and 2.6 Ga (**Figure 7**) have been interpreted by some workers (Ohmoto et al. 2006, Ono et al. 2006) to suggest that a rise in atmospheric O_2 occurred prior to the Great Oxidation Event at ~2.4 Ga (Holland 1984), reflecting a yo-yo atmospheric evolution. Other workers have countered that despite the small $\Delta^{33}S$ values for sedimentary rocks of ~2.9 to 2.6 Ga age, small mass-independent S isotope fractionations still exist, indicating that atmospheric O_2 contents must have been low (Farquhar et al. 2007). In contrast, new Mo isotope data have been interpreted to reflect a gradual rise in O_2 from 2.65 to 2.5 Ga based on increasingly fractionated $^{98}Mo/^{95}Mo$ ratios up section in black shales of the Transvaal Supergroup, which Wille et al. (2007) have interpreted to reflect increasingly mobile Mo in solution (as oxyanions) with time, requiring relatively oxic conditions, at least in seawater. New Mo and Re concentration and multiple S isotope data for the 2.5 Ga Mount McRae Shale (Australia) have been interpreted to reflect a small increase in free O_2 in at least the surface oceans before the Great Oxidation Event at ~2.4 Ga (Anbar et al. 2007, Kaufman et al. 2007), although the timing of this proposed increase is significantly younger than that proposed by Ohmoto et al. (2006), Ono et al. (2006), and Wille et al. (2007).

Strikingly, the $\delta^{56}Fe$ values for sedimentary pyrite and C- and/or S-rich shales drop to the lowest values yet measured on Earth between ~2.7 and 2.5 Ga (**Figure 7**), and we propose that this reflects an extensive radiation in DIR in response

to increased Fe^{3+} and organic carbon delivery to the oceans. Oxygenic photosynthesis would be the most efficient means for producing the high Fe^{3+} and organic carbon fluxes that are required to support extensive DIR, and given the balance of arguments for and against free O_2 between ~2.7 and 2.5 Ga summarized above, we suggest that local oxidation of Fe^{2+} in the surface oceans by oxygenic photosynthesis is a plausible mechanism for providing the raw materials to support DIR. This model is similar to that of Beukes et al. (1990), who suggested that oxidation of Fe^{2+} occurred in the upper water column during BIF formation, reflecting localized enrichment in free O_2 from oxygenic photosynthesis; anaerobic photosynthetic Fe^{2+} oxidation is an alternative explanation (e.g., Kappler et al. 2005). Local enrichment of the surface ocean in oxygen may have supported BSR, and Archer & Vance (2006) argued that coupled BSR and DIR are recorded in the correlated variation in $\delta^{34}S$ and $\delta^{56}Fe$ values of sedimentary pyrite from the 2.7 Ga Belingwe sedimentary basin (**Figure 7*b***, inset).

Our model does not require relatively high levels of atmospheric O_2 because oxygen enrichment in the surface ocean could occur if the atmosphere was anoxic, although an O_2-bearing atmosphere is certainly permitted by our model. As highlighted by numerous studies (e.g., Catling & Claire 2005, Claire et al. 2006, Goldblatt et al. 2006, Kump & Barley 2007), atmospheric O_2 contents could have risen only after all sinks for oxygen had been exhausted. Indeed, modeling of the balances between sources and sinks can produce a yo-yo atmosphere in terms of O_2 contents prior to the Great Oxidation Event (e.g., Goldblatt et al. 2006) or a single pulse of slightly increased atmospheric O_2 between ~2.7 Ga and 2.5 Ga (e.g., Claire et al. 2006). One of the most important sinks was the inventory of Fe^{2+} that existed in the oceans and the continents, providing a tie to the Fe isotope record. Consideration of the importance of Fe^{2+} sinks predicts that Fe^{3+} inventories will increase before an increase in atmospheric O_2, which in turn will increase DIR activity prior to a rise in atmospheric O_2, and this is consistent with the large range in $\Delta^{33}S$ values that are found during the time of large excursions in $\delta^{56}Fe$ values (**Figure 7**).

There is essentially no debate that atmospheric O_2 contents were relatively high after ~2.4 Ga (e.g., Bekker et al. 2004). Oxygenic photosynthesis was well established by this time, producing moderately negative $\delta^{13}C$ values for organic carbon (**Figure 7**) and seawater SO_4^{2-} contents significantly increased (Habicht et al. 2002), as reflected in the expanded range in $\delta^{34}S$ values for sedimentary pyrite (**Figure 7**). The Fe isotope record suggests that DIR became much less extensive (**Figure 7**). Once SO_4^{2-} contents in the oceans increased to relatively high levels at ~2.4 Ga, sulfide abundances greatly restricted DIR in open-ocean environments because sulfide would scavenge reactive Fe^{3+} through reaction of ferric oxide/hydroxides and sulfide to form Fe sulfides, preventing its availability for DIR; at this time, we suggest that DIR became restricted to oxic/anoxic interfaces in marine sediments in which sulfide contents were low, as is the case today. The near-zero to slightly positive $\delta^{56}Fe$ values for C-, and/or S-rich shales, sedimentary pyrite, and magnetite from BIFs in the post −2.4 Ga period are strikingly similar to those measured for early Archean rocks, although there seems little doubt that the surface conditions on Earth must have been quite different between these two time periods. Canfield (1998) proposed that cessation of BIF deposition at ~1.8 Ga reflected the removal of Fe^{2+}_{aq} by high sulfide

contents in the deep ocean, rather than the traditional interpretation that the deep oceans became oxygenated. The transition to a sulfidic ocean following cessation of BIF deposition has been demonstrated in the rock record (Poulton et al. 2004). We interpret the near-zero δ^{56}Fe values to record complete oxidation and precipitation of hydrothermal Fe^{2+}_{aq}, as would be expected under an O_2-bearing atmosphere. In addition, sedimentary pyrite that formed through sulfidation of detrital Fe^{3+}, which should have $\delta^{56}Fe \sim 0‰$, is another explanation for near-zero δ^{56}Fe values for sedimentary pyrite. If, however, significant Fe was titrated by sulfide as FeS in the deeper parts of the oceans, it is possible that the remaining Fe^{2+}_{aq} in the upper ocean layer had slightly positive δ^{56}Fe values, given the slightly positive Fe^{2+}_{aq}-FeS fractionations measured in experiment (Butler et al. 2005). There are some difficulties with this interpretation because it predicts that pyrite formed directly from low-δ^{56}Fe FeS precursors in the deep ocean would have slightly negative δ^{56}Fe values, and such compositions are rare during this time interval (**Figure 7**).

CONCLUSIONS AND FUTURE DIRECTIONS

Significant Fe isotope fractionations are largely restricted to natural, low-temperature environments or processes in which redox or bonding changes occur, and these fractionations can only be expressed in systems in which one or more Fe species can be mobilized. In modern Earth, these conditions are satisfied by the complexation of soluble Fe in soils, rivers, and seawater, as well as marine hydrothermal alteration, the oxidation of reduced hot springs and groundwaters, and microbial Fe cycling in marine sediments. In terms of processes that produce the largest quantities of isotopically distinct Fe, DIR appears to be most important by an order of magnitude or more. Abiologic processes commonly proposed to produce fractionated isotope compositions for aqueous Fe such as sorption or partial oxidation and precipitation are inadequate for producing large inventories of isotopically fractionated Fe. The total inventory of Fe that has δ^{56}Fe values significantly different than the crust, however, is quite small in Earth today.

The pools of reduced and oxidized Fe mobilized in the early Proterozoic and Archean must have been much larger than today to explain the significant inventory of bulk sedimentary rocks and minerals that have nonzero δ^{56}Fe values. The temporal isotopic record in Precambrian rocks reflects changes in the specific microbial metabolisms that cycled C, S, and Fe. Some workers have argued that the temporal changes in the Fe isotope record reflect abiologic processes, arguing that the quantities of Fe processed by microbes would be too small relative to abiologic processes (Rouxel et al. 2005, Dauphas & Rouxel 2006, Anbar & Rouxel 2007), but the data at hand suggest that the opposite is the case. The recognized importance of DIR as an early form of microbial metabolism (e.g., Vargas et al. 1998, Lovley 2004), together with correlations between C, S, and Fe isotopes, provide us with a view into the inter-relations between photosynthesis and bacterial sulfate and iron reduction as a function of changing surface environments in ancient Earth. The fundamental importance of photosynthesis in defining the Precambrian Fe and S isotope records

lies in its role in producing a sustained and large flux of the Fe^{3+}, SO_4^{2-}, and organic carbon that are required to fuel DIR and BSR.

The earliest Fe isotope record in early Archean rocks suggests that incomplete oxidation of marine Fe^{2+}_{aq} occurred by anaerobic photosynthetic Fe^{2+} oxidation, which produced Fe oxides in BIFs that had positive $\delta^{56}Fe$ values, as well as negative $\delta^{13}C$ values for organic carbon. The Fe isotope record significantly changes at ~3.1 Ga, at which the combination of an increase in production of organic carbon via photosynthesis and an increase in reactive Fe^{3+} provided the raw materials needed for a widespread radiation of DIR that peaked between ~2.7 Ga and 2.5 Ga. An increased flux of mantle Fe into the oceans in the late Archean may have enhanced Fe cycling, ultimately reflecting widespread submarine volcanism and hydrothermal activity prior to continental stabilization at the end of the Archean (e.g., Davies 1995, Barley et al. 1998). The radiation of DIR in the late Archean was possible in part because seawater SO_4^{2-} contents remained relatively low during this time, as evidenced by the generally modest spread in $\delta^{34}S$ values during this time interval. BSR, however, could not have been nonexistent, given the modest range in $\delta^{34}S$ values, and the low-$\delta^{56}Fe$ values for pyrite that are found in this time interval are interpreted to reflect the interaction between sulfide produced by BSR and Fe^{2+}_{aq} produced by DIR (Archer & Vance 2006).

The very large BIF deposits formed at ~2.5 Ga involved a major component of biogeochemical cycling, in which photosynthesis in the upper water column provided organic carbon fluxes to the deep oceans, as well as a means to oxidize Fe^{2+}_{aq}, either by oxygenic photosynthesis or by anaerobic photosynthetic Fe^{2+} oxidation (e.g., Kappler et al. 2005). The rain of Fe^{3+} oxide as well as organic carbon from the upper water column to the ocean floor provided the essential ingredients to support DIR during BIF genesis at this time, as proposed in the geomicrobiology literature (e.g., Lovley et al. 1987, Nealson & Myers 1990, Konhauser et al. 2005). This flux would have sustained a condition of partial iron oxide reduction by DIR, producing large quantities of Fe^{2+}_{aq} that had negative $\delta^{56}Fe$ values, much in the same way that negative $\delta^{34}S$ values of sedimentary sulfides have been interpreted to reflect BSR in the presence of excess sulfate (e.g., Canfield 2001). The rise in SO_4^{2-} between ~2.5 and 2.4 Ga, however, caused DIR to become more restricted in extent, producing a concomitant shift in the Fe isotope record toward average crustal values. The transition to a sulfidic ocean at ~1.8 Ga, which appears to have been accompanied by the cessation of BIF deposition (Canfield 1998), produced Fe isotope compositions for sulfides that were close to the crustal average, reflecting the sulfidation of detrital Fe^{3+} or Fe^{3+} produced by the complete oxidation of hydrothermal Fe^{2+} under an oxic atmosphere. It is important to note, however, that the presence of an oxygenated atmosphere does not require that all marine sedimentary rocks must have near-zero $\delta^{56}Fe$ values, and this is well demonstrated by the large fluctuation in Fe isotope compositions that is associated with the Cenomanian-Turonian oceanic anoxic event (Jenkyns et al. 2007), which provides strong support for the concept that microbial metabolisms exert a stronger control on the Fe isotope record of marine sediments than ambient atmospheric oxygen contents.

Although the phylogenetic importance of DIR has been recognized for the past two decades (Lovley et al. 1987, Myers & Nealson 1988), this metabolism has received relatively little attention in discussions in the isotope geochemical literature relative to photosynthesis and sulfate reduction, primarily because the isotopic record for DIR has only recently emerged. Future research is required to increase our understanding of the isotopic fractionations produced by DIR in natural, complex aqueous systems such as seawater and to compare these fractionations with those that arise from abiologic Fe^{2+}-oxide interactions. In the rock record, it is clear that testing the proposal that the C, S, and Fe isotope records are isotopically coupled through photosynthesis and heterotrophic respiration requires detailed studies of these isotope compositions on the same samples, including mass-independent S isotope measurements. The large number of negative $\delta^{56}Fe$ values measured in the rock record as it is currently known presents a puzzle, given the mass-balance constraints provided by the homogeneity of igneous and average crustal Fe. Because the Fe isotope record for Precambrian sedimentary rocks is so far based on a limited number of samples that probably give an incomplete picture of the environments that existed at any particular time, we suspect that our understanding of Fe biogeochemical cycling will improve by basin-scale studies, comparing both shallow-water and deep-water environments, an approach used, for example, in C isotope studies (e.g., Eigenbrode & Freeman 2006). If accompanied by a significant expansion in experimental studies to provide a mechanistic understanding of isotopic fractionations, we are confident that in the coming decade C, S, and Fe isotope studies on the same samples will provide important insights into the coupled C-S-Fe biogeochemical cycles in early Earth.

DISCLOSURE STATEMENT

The authors are not aware of any biases that might be perceived as affecting the objectivity of this review.

ACKNOWLEDGMENTS

Financial support for our Fe isotope research over the years has been provided by NASA and the NSF. Many of the ideas in this paper have their roots in collaborations with Nic Beukes, Nan-Chin Chu, Laura Croal, Heidi Crosby, Chris German, Morgan Herrick, Andreas Kappler, Chris Kennedy, Kase Klein, Jim McManus, Ken Nealson, Dianne Newman, Hiroshi Ohmoto, Rebecca Poulson, Silke Severmann, Joe Skulan, Sue Welch, Rene Wiesli, and Kosei Yamaguchi. In addition, we wish to acknowledge the important contributions of Don Canfield and his collaborators in paving the way for an integrated view of the isotopic record of C-S-Fe cycling that formed a fundamental framework for the interpretations we present here. Finally, Jochen Brocks, Roger Buick, James Farquhar, Tim Lyons, Alan Matthews, and Martin van Kranendonk are thanked for important comments on the manuscript that substantially improved this review.

LITERATURE CITED

Anbar AD. 2004. Iron stable isotopes: beyond biosignatures. *Earth Planet. Sci. Lett.* 217:223–46

Anbar AD, Duan Y, Lyons TW, Arnold GL, Kendall B, et al. 2007. A whiff of oxygen before the great oxidation event? *Science* 317:1903–6

Anbar AD, Jarzecki AA, Spiro TG. 2005. Theoretical investigation of iron isotope fractionation between $Fe(H_2O)_6^{3+}$ and $Fe(H_2O)_6^{2+}$: implications for iron stable isotope geochemistry. *Geochim. Cosmochim. Acta* 69:825–37

Anbar AD, Roe JE, Barling J, Nealson KH. 2000. Nonbiological fractionation of iron isotopes. *Science* 288:126–28

Anbar AD, Rouxel O. 2007. Metal stable isotopes in paleoceanography. *Annu. Rev. Earth Planet. Sci.* 35:717–46

Archer C, Vance D. 2006. Coupled Fe and S isotope evidence for Archean microbial Fe(III) and sulfate reduction. *Geology* 34:153–56

Barley ME, Krapez B, Groves DI, Kerrich R. 1998. The Late Archean bonanza: metallogenic and environmental consequences of the interactions between mantle plumes, lithospheric tectonics and global cyclicity. *Precamb. Res.* 91:65–90

Beard BL, Johnson CM. 2004. Fe isotope variations in the modern and ancient earth and other planetary bodies. *Rev. Mineral. Geochem.* 55:319–57

Beard BL, Johnson CM, Cox L, Sun H, Nealson KH, Aguilar C. 1999. Iron isotope biosignatures. *Science* 285:1889–92

Beard BL, Johnson CM, Nealson KH. 1998. Precise iron isotopic measurements reveals naturally occurring, mass-dependent iron isotope fractionations. *Geol. Soc. Am. Abstr. Programs* 30:A157

Beard BL, Johnson CM, Skulan JL, Nealson KH, Cox L, Sun H. 2003a. Application of Fe isotopes to tracing the geochemical and biological cycling of Fe. *Chem. Geol.* 195:87–117

Beard BL, Johnson CM, Von Damm KL, Poulson RL. 2003b. Iron isotope constraints on Fe cycling and mass balance in oxygenated Earth oceans. *Geology* 31:629–32

Bekker A, Holland HD, Wang PL, Rumble D, Stein HJ, et al. 2004. Dating the rise of atmospheric oxygen. *Nature* 427:117–20

Benning LG, Wilkin RT, Barnes HL. 2000. Reaction pathways in the Fe-S system below 100°C. *Chem. Geol.* 167:25–51

Bergquist BA, Boyle EA. 2006. Iron isotopes in the Amazon River system: weathering and transport signatures. *Earth Planet. Sci. Lett.* 248:54–68

Beukes NJ, Klein C, Kaufman AJ, Hayes JM. 1990. Carbonate petrography, kerogen distribution, and carbon and oxygen isotope variations in an early Proterozoic transition from limestone to iron-formation deposition, Transvaal Supergroup, South Africa. *Econ. Geol.* 85:663–90

Bjerrum CJ, Canfield DE. 2002. Ocean productivity before about 1.9 Gyr limited by phosphorus adsorption onto iron oxides. *Nature* 417:159–62

Bjerrum CJ, Canfield DE. 2004. New insights into the burial history of organic carbon on the early Earth. *Geochem. Geophys. Geosys.* 5:doi:10.1029/2004GC000713

Boetius A, Ravenschlag K, Schubert CJ, Rickert D, Widdel F, et al. 2000. A marine microbial consortium apparently mediating anaerobic oxidation of methane. *Nature* 407:623–26

Bosak T, Greene SE, Newman DK. 2007. A likely role for anoxygenic photosynthetic microbes in the formation of ancient stromatolites. *Geobiology* 5:119–26

Brantley SL, Liermann L, Bullen TD. 2001. Fractionation of Fe isotopes by soil microbes and organic acids. *Geology* 29:535–38

Brantley SL, Liermann LJ, Guynn RL, Anbar A, Icopini GA, Barling J. 2004. Fe isotopic fractionation during mineral dissolution with and without bacteria. *Geochim. Cosmochim. Acta* 68:3189–204

Brasier MD, Green OR, Jephcoat AP, Kleppe AK, van Kranendonk MJ, et al. 2002. Questioning the evidence for Earth's oldest fossils. *Nature* 416:76–81

Braterman PS, Cairnssmith AG. 1987. Photoprecipitation and the banded iron formations: some quantitative aspects. *Orig. Life Evol. Biosph.* 17:221–28

Brocks JJ, Buick R, Summons RE, Logan GA. 2003. A reconstruction of Archean biological diversity based on molecular fossils from the 2.78 to 2.45 billion-year-old Mount Bruce Supergroup, Hamersley Basin, Western Australia. *Geochim. Cosmochim. Acta* 67:4321–35

Brocks JJ, Grosjean E, Logan GA. 2008. Assessing biomarker syngeneity using branched alkanes with quaternary carbon (BAQCs) and other plastic contaminants. *Geochim. Cosmochim. Acta.* 72:871–88

Brocks JJ, Logan GA, Buick R, Summons RE. 1999. Archean molecular fossils and the early rise of eukaryotes. *Science* 285:1033–36

Bullen TD, McMahon PB. 1998. Using stable Fe isotopes to assess microbially mediated Fe^{3+} reduction in a jet-fuel contaminated aquifer. *Mineral. Mag.* 62:A255–56

Bullen TD, White AF, Childs CW, Vivit DV, Schulz MS. 2001. Demonstration of significant abiotic iron isotope fractionation in nature. *Geology* 29:699–702

Butler IB, Archer C, Vance D, Oldroyd A, Rickard D. 2005. Fe isotope fractionation on FeS formation in ambient aqueous solution. *Earth Planet. Sci. Lett.* 236:430–42

Canfield DE. 1998. A new model for Proterozoic ocean chemistry. *Nature* 396:450–53

Canfield DE. 2001. Biogeochemistry of sulfur isotopes. *Rev. Mineral. Geochem.* 43:607–36

Canfield DE. 2005. The early history of atmospheric oxygen: homage to Robert Garrels. *Annu. Rev. Earth Planet. Sci.* 33:1–36

Canfield DE, Jorgensen BB, Fossing H, Glud R, Gundersen J, et al. 1993a. Pathways of organic-carbon oxidation in three continental margin sediments. *Mar. Geol.* 113:27–40

Canfield DE, Kristensen E, Thamdrup B. 2005. *Aquatic Geomicrobiology*. San Diego: Academic. 640 pp.

Canfield DE, Rosing MT, Bjerrum C. 2006. Early anaerobic metabolisms. *Philos. Trans. R. Soc. London B* 361:1819–36

Canfield DE, Thamdrup B, Hansen JW. 1993b. The anaerobic degradation of organic matter in Danish coastal sediments: iron reduction, manganese reduction, and sulfate reduction. *Geochim. Cosmochim. Acta* 57:3867–83

Catling DC, Claire MW. 2005. How Earth's atmosphere evolved to an oxic state: a status report. *Earth Planet. Sci. Lett.* 237:1–20
Claire MW, Catling DC, Zahnle KJ. 2006. Biogeochemical modeling of the rise in atmospheric oxygen. *Geobiology* 4:239–69
Criss RE. 1999. *Principles of Stable Isotope Distribution*. New York: Oxford Univ. Press
Croal LR, Johnson CM, Beard BL, Newman DK. 2004. Iron isotope fractionation by Fe(II)-oxidizing photoautotrophic bacteria. *Geochim. Cosmochim. Acta* 68:1227–42
Crosby HA. 2005. *Mechanisms of iron isotope fractionation during dissimilatory iron reduction and Fe(II) adsorption*. MS thesis. Univ. Wis., Madison. 60 pp.
Crosby HA, Johnson CM, Roden EE, Beard BL. 2005. Coupled Fe(II)-Fe(III) electron and atom exchange as a mechanism for Fe isotope fractionation during dissimilatory iron oxide reduction. *Environ. Sci. Technol.* 39:6698–704
Crosby HA, Roden EE, Johnson CM, Beard BL. 2007. The mechanisms of iron isotope fractionation produced during dissimilatory Fe(III) reduction by *Shewanella putrefaciens* and *Geobacter sulfurreducens*. *Geobiology* 5:169–89
Dauphas N, Cates NL, Mojzsis SJ, Busigny V. 2007. Identification of chemical sedimentary protoliths using iron isotopes in the >3750 Ma Nuvvuagittuq supracrustal belt, Canada. *Earth Planet. Sci. Lett.* 254:358–76
Dauphas N, Rouxel O. 2006. Mass spectrometry and natural variations in iron isotopes. *Mass Spectrom. Rev.* 25:515–50
Dauphas N, van Zuilen M, Wadhwa M, Davic AM, Marty B, Janney PE. 2004. Clues from Fe isotope variations on the origin of Early Archean BIFs from Greenland. *Science* 306:2077–80
Davies GF. 1995. Punctuated tectonic evolution of the earth. *Earth Planet. Sci. Lett.* 136:363–79
Des Maris DJ. 2000. When did photosynthesis emerge on Earth? *Science* 289:1703–5
Des Marais DJ. 2001. Isotopic evolution of the biogeochemical carbon cycle during the Precambrian. *Rev. Mineral. Geochem.* 43:555–78
DiChristina TJ, Fredrickson JK, Zachara JM. 2005. Enzymology of electron transport: energy generation with geochemical consequences. *Rev. Mineral. Geochem.* 59:27–52
Eigenbrode JL, Freeman KH. 2006. Late Archean rise of aerobic microbial ecosystems. *Proc. Natl. Acad. Sci. USA* 43:15759–64
Emmanuel S, Erel Y, Matthews A, Teutsch N. 2005. A preliminary mixing model for Fe isotopes in soils. *Chem. Geol.* 222:23–34
Ewers WE. 1983. Chemical factors in the deposition and diagenesis of banded iron-formation. In *Iron Formations: Facts and Problems*, ed. AF Trendall, RC Morris, pp. 491–512. Amsterdam: Elsevier
Fantle MS, DePaolo DJ. 2004. Iron isotopic fractionation during continental weathering. *Earth Planet. Sci. Lett.* 228:547–62
Farquhar J, Peters M, Johnston DT, Strauss H, Masterson A, et al. 2007. Isotopic evidence for Mesoarchaean anoxia and changing atmospheric sulphur chemistry. *Nature* 449:706–9
Farquhar J, Wing BA. 2003. Multiple sulfur isotopes and the evolution of the atmosphere. *Earth Planet. Sci. Lett.* 213:1–13

Frost CD, von Blanckenburg F, Schoenberg R, Frost BR, Swapp SM. 2006. Preservation of Fe isotope heterogeneities during diagenesis and metamorphism of banded iron formation. *Contrib. Mineral. Petrol.* 153:211–35

Goldblatt C, Lenton TM, Watson AJ. 2006. Bistability of atmospheric oxygen and the Great Oxidation. *Nature* 443:683–86

Gorby YA, Svetlana Y, McLean JS, Rosso KM, Moyles D, et al. 2007. Electrically conductive bacterial nanowires produced by *Shewanella oneidensis* strain MR-1 and other microorganisms. *Proc. Natl. Acad. Sci. USA* 103:11358–63

Grassineau NV, Nisbet EG, Bickle MJ, Fowler CM, Lowry D, et al. 2001. Antiquity of the biological sulphur cycle: evidence from sulphur and carbon isotopes in 2700 million-year-old rocks of the Belingwe Belt, Zimbabwe. *Proc. Biol. Sci.* 268:113–19

Habicht KS, Gade M, Thampdrup B, Berg P, Canfield DE. 2002. Calibration of sulfate levels in the Archean ocean. *Science* 298:2372–74

Hayes JM. 1983. Geochemical evidence bearing on the origin of aerobiosis: a speculative hypothesis. In *Earth's Earliest Biosphere: Its Origin and Evolution*, ed. JW Schopf, pp. 291–301. Princeton, NJ: Princeton Univ. Press

Hayes JM. 2001. Fractionation of carbon and hydrogen isotopes in biosynthetic processes. *Rev. Mineral. Geochem.* 43:225–77

Hayes JM, Takigiku R, Ocampo R, Callot HJ, Albrecht P. 1987. Isotopic compositions and probable origin of organic molecules in the Eocene Messle shale. *Nature* 329:48–51

Hayes JM, Waldbauer JR. 2006. The carbon cycle and associated redox processes through time. *Philos. Trans. R. Soc. B* 361:931–50

Herrick M. 2007. *Iron isotopes provide insight into the earliest Fe geochemical cycles on Earth at Isua, SW Greenland*. MS thesis. Univ. Wis., Madison

Hinrichs KU. 2002. Microbial fixation of methane carbon at 2.7 Ga: Was an anaerobic mechanism possible? *Geochm. Geophys. Geosys.* 3:doi:10.1029/2001GC000286

Hinrichs KU, Hayes JM, Sylva SP, Brewer PG, DeLong EF. 1999. Methane-consuming archaebacteria in marine sediments. *Nature* 398:802–5

Holland HD. 1984. *The Chemical Evolution of the Atmosphere and Oceans*. Princeton, NJ: Princeton Univ. Press. 582 pp.

Hyslop EV, Valley JW, Johnson CM, Beard BL. 2008. The effects of metamorphism on O and Fe isotope compositions in the Biwabik Iron Formation, northern Minnesota. *Contrib. Mineral. Petrol.* 155:313–28

Icopini GA, Anbar AD, Ruebush SS, Tien M, Brantley SL. 2004. Iron isotope fractionation during microbial reduction of iron: the importance of adsorption. *Geology* 32:205–8

Jenkyns HC, Matthews A, Tsikos H, Erel Y. 2007. Nitrate reduction, sulfate reduction and sedimentary iron-isotope evolution during the Cenomanian-Turonian Anoxic Event. *Paleoceanography* 22:PA3208

Johnson CM, Beard BL. 2006. Fe isotopes: an emerging technique in understanding modern and ancient biogeochemical cycles. *GSA Today* 16:4–10

Johnson CM, Beard BL, Beukes NJ, Klein C, O'Leary JM. 2003. Ancient geochemical cycling in the Earth as inferred from Fe isotope studies of banded iron formations from the Transvaal Craton. *Contrib. Miner. Petrol.* 144:523–47

Johnson CM, Beard BL, Klein C, Beukes NJ, Roden EE. 2008. Iron isotopes constrain biologic and abiologic processes in Banded Iron Formation genesis. *Geochim. Cosmochim. Acta.* 72:151–69

Johnson CM, Beard BL, Roden EE, Newman DK, Nealson KH. 2004. Isotopic constraints on biogeochemical cycling of Fe. *Rev. Mineral. Geochem.* 55:359–408

Johnson CM, Roden EE, Welch SA, Beard BL. 2005. Experimental constraints on Fe isotope fractionation during magnetite and Fe carbonate formation coupled to dissimilatory hydrous ferric oxide reduction. *Geochim. Cosmochim. Acta* 69:963–93

Johnson CM, Skulan JL, Beard BL, Sun H, Nealson KH, Braterman PS. 2002. Isotopic fractionation between Fe(III) and Fe(II) in aqueous solutions. *Earth Planet. Sci. Lett.* 195:141–53

Kappler A, Pasquero C, Konhauser KO, Newman DK. 2005. Deposition of banded iron formations by anoxygenic phototrophic Fe(II)-oxidizing bacteria. *Geology* 33:865–68

Kaufman AJ, Johnston DT, Farquhar J, Masterson AL, Lyons TW, et al. 2007. Late Archean biospheric oxygenation and atmospheric evolution. *Science* 317:1900–3

Kasting JF, Holland HD, Kump LR. 1992. Atmospheric evolution: the rise of oxygen. In *The Proterozoic Biosphere*, ed. JW Schopf, C Klein, pp. 159–63. New York: Cambridge Univ. Press

Kennedy CB, Crosby HA, Beard BL, Roden EE, Johnson CM. 2006. Iron isotope fractionation during Fe(II)-hematite interactions. *AGU EOS Trans. Fall Meet. Suppl.* 2006:B13B-1094

Klein C. 2005. Some Precambrian banded iron formations (BIFs) from around the world: their age, geologic setting, mineralogy, metamorphism, geochemistry, and origin. *Am. Mineral.* 90:1473–99

Konhauser KO, Amskold L, Lalonde SV, Posth NR, Kappler A, Anbar A. 2007. Decoupling photochemical Fe(II) oxidation from shallow-water BIF deposition. *Earth Planet. Sci. Lett.* 258:87–100

Konhauser KO, Newman DK, Kappler A. 2005. The potential significance of microbial Fe(III) reduction during deposition of Precambrian banded iron formations. *Geobiology* 3:167–77

Kopp RE, Kirschvink JL, Hilburn IA, Nash CZ. 2005. The Paleoproterozoic snowball Earth: a climate disaster triggered by the evolution of oxygenic photosynthesis. *Proc. Natl. Acad. Sci. USA* 32:11131–36

Kukkadapu RK, Zachara JM, Fredrickson JK, Kennedy DW. 2004. Biotransformation of two-line silica-ferrihydrite by a dissimilatory Fe(III)-reducing bacterium: formation of carbonate green rust in the presence of phosphate. *Geochim. Cosmochim. Acta* 68:2799–814

Kump LR, Barley ME. 2007. Increased subaerial volcanism and the rise of atmospheric oxygen 2.5 billion years ago. *Nature* 448:1033–36

Kump LR, Holland HD. 1992. Iron in Precambrian rocks: implications for the global oxygen budget of the ancient Earth. *Geochim. Cosmochim. Acta* 56:3217–23

Lecuyer C, Ricard Y. 1999. Long-term fluxes and budget of ferric iron: implication for the redox states of the Earth's mantle and atmosphere. *Earth Planet. Sci. Lett.* 165:197–211

Levasseur S, Frank M, Hein JR, Halliday AN. 2004. The global variation in the iron isotope composition of marine hydrogenetic ferromanganese deposits: implications for seawater chemistry? *Earth Planet. Sci. Lett.* 224:91–105

Londry KL, Des Marais DJ. 2003. Stable carbon isotope fractionation by sulfate-reducing bacteria. *Appl. Environ. Microbiol.* 69:2942–49

Lovley DR. 2004. Potential role of dissimilatory iron reduction in the early evolution of microbial respiration. In *Origins, Evolution, and Biodiversity of Microbial Life*, ed. J Seckbach, pp. 301–13. Amsterdam: Kluwer

Lovley DR, Holmes DE, Nevin KP. 2004. Dissimilatory Fe(III) and Mn(IV) reduction. *Adv. Microb. Physiol.* 49:219–86

Lovley DR, Phillips EJP. 1987. Competitive mechanism for inhibition of sulfate reduction and methane production in the zone of ferric iron reduction in sediments. *Appl. Environ. Microbiol.* 53:2636–41

Lovley DR, Phillips EJP. 1988. Novel mode of microbial energy metabolism: organic carbon oxidation coupled to dissimilatory reduction of iron or manganese. *Appl. Environ. Microbiol.* 54:1472–80

Lovley DR, Stolz JF, Nord GL, Phillips EJP. 1987. Anaerobic production of magnetite by a dissimilatory iron-reducing microorganism. *Nature* 330:252–44

Lower SK, Hochella MF Jr, Beveridge TJ. 2001. Bacterial recognition of mineral surfaces: nanoscale interactions between *Shewanella* and α-FeOOH. *Science* 1360–63

Lower BH, Shi L, Yongsunthon R, Droubay TC, McCready DE, Lower SK. 2007. Specific bonds between an iron oxide surface and outer membrane cytochromes MtrC and OmcA from *Shewanella oneidensis* MR-1. *J. Bacteriol.* 189:4944–52

Matthews A, Morgans-Bell HS, Emmanuel S, Jenkyns HC, Erel Y, Halicz L. 2004. Controls on iron-isotope fractionation in organic-rich sediments (Kimmeridge Clay, Upper Jurassic, southern England). *Geochim. Cosmochim. Acta* 68:3107–23

Myers CR, Nealson KH. 1988. Bacterial manganese reduction and growth with manganese oxide as the sole electron acceptor. *Science* 240:1319–21

Nealson KH, Myers CR. 1990. Iron reduction by bacteria: a potential role in the genesis of banded iron formations. *Am. J. Sci.* 290:A35–45

Ohmoto H, Watanabe Y, Ikemi H, Poulson SR, Taylor BE. 2006. Sulfur isotope evidence for an oxic Archean atmosphere. *Nature* 442:908–11

Olson JM. 2006. Photosynthesis in the Archean Era. *Photosynth. Res.* 88:109–17

Ono S, Beukes NJ, Rumble D, Fogel ML. 2006. Early evolution of atmospheric oxygen from multiple-sulfur and carbon isotope records of the 2.9 Ga Mozaan Group of the Pongola Supergroup, Southern Africa. *S. Afr. J. Geol.* 109:97–108

Orphan VJ, House CJ, Hinrichs KU, McKeegan KD, DeLong EF. 2002. Multiple archaeal groups mediate methane oxidation in anoxic cold seep sediments. *Proc. Natl. Acad. Sci. USA* 99:7663–68

Pedersen HD, Postma D, Jakobsen R, Larsen O. 2005. Fast transformation of iron oxyhydroxides by the catalytic action of aqueous Fe(II). *Geochim. Cosmochim. Acta* 69:3967–77

Philippot P, van Zuilen M, Lepot K, Thomazo C, Farquhar J, Van Kranendonk MJ. 2007. Early Archaean microorganisms preferred elemental sulfur, not sulfate. *Science* 317:1534–37

Poitrasson F, Halliday AN, Lee DC, Levasseur S, Teutsch N. 2004. Iron isotope differences between Earth, Moon, Mars and Vesta as possible records of contrasted accretion mechanisms. *Earth Planet. Sci. Lett.* 223:253–66

Polyakov VB, Clayton RA, Horita J, Mineev SD. 2007. Equilibrium iron isotope fractionation factors of minerals: reevaluation from the data of nuclear inelastic resonant X-ray scattering and Mössbauer spectroscopy. *Geochim. Cosmochim. Acta* 71:3833–46

Polyakov VB, Mineev SD. 2000. The use of Mössbauer spectroscopy in stable isotope geochemistry. *Geochim. Cosmochim. Acta* 64:849–65

Poulson RL. 2005. *Iron isotope variations as tracers for iron geochemical cycling: investigating the behavior of aqueous and precipitated iron species in natural and synthetic systems*. MS thesis. Univ. Wis., Madison. 87 pp.

Poulton SW, Fralick PW, Canfield DE. 2004. The transition to a sulfidic ocean ~1.84 billion years ago. *Nature* 431:173–77

Poulton SW, Raiswell R. 2002. The low-temperature geochemical cycle of iron: from continental fluxes to marine sediment deposition. *Am. J. Sci.* 302:774–805

Reguera G, McCarthy K, Mehta T, Nicoll J, Tuominen M, Lovley D. 2005. Extracellular electron transfer via microbial nanowires. *Nature* 435:1098–101

Rickard DT, Luther GW. 1997. Kinetics of pyrite formation by the H2S oxidation of iron(II) monosulfide in aqueous solutions between 25 and 125°C: the mechanism. *Geochim. Cosmochim. Acta* 61:135–47

Romanek CS, Zhang CL, Li Y, Horita J, Vali H, et al. 2003. Carbon and hydrogen isotope fractionations associated with dissimilatory iron-reducing bacteria. *Chem. Geol.* 195:5–16

Rosing MT, Bird DK, Sleep NH, Glassley W, Albarede F. 2006. The rise of continents—an essay on the geologic consequences of photosynthesis. *Palaeogeog. Palaeclim. Palaeoecol.* 232:99–113

Rosing MT, Frei R. 2004. U-rich Archaean sea-floor sediments from Greenland—indications of >3700 Ma oxygenic photosynthesis. *Earth Planet. Sci. Lett.* 217:237–44

Rouxel OJ, Bekker A, Edwards KJ. 2005. Iron isotope constraints on the Archean and Paleoproterozoic ocean redox state. *Science* 307:1088–91

Rouxel OJ, Bekker A, Edwards KJ. 2006. Response to comment on "Iron isotope constraints on the archean and paleoproterozoic ocean redox state." *Science* 311:177

Schauble EA. 2004. Applying stable isotope fractionation theory to new systems. *Rev. Mineral. Geochem.* 55:65–111

Schauble EA, Rossman GR, Taylor HP. 2001. Theoretical estimates of equilibrium Fe-isotope fractionations from vibrational spectroscopy. *Geochim. Cosmochim. Acta* 65:2487–97

Schidlowski M. 2001. Carbon isotopes as biogeochemical recorders of life over 3.8 Ga of Earth history: evolution of a concept. *Precambr. Res.* 106:117–34

Schoonen MAA. 2004. Mechanisms of sedimentary pyrite formation. *Geol. Soc. Am. Spec. Pap.* 379:117–33

Schopf JW. 1993. Microfossils of the early Archean Apex chert: new evidence of the antiquity of life. *Science* 260:640–46

Severmann S, Johnson CM, Beard BL, German CR, Edmonds HN, et al. 2004. The effect of plume processes on the Fe isotope composition of hydrothermally derived Fe in the deep ocean as inferred from the Rainbow vent site, Mid-Atlantic Ridge, 36° 14′ N. *Earth Planet. Sci. Lett.* 225:63–76

Severmann S, Johnson CM, Beard BL, McManus J. 2006. The effect of early diagenesis on the Fe isotope compositions of porewaters and authigenic minerals in continental margin sediments. *Geochim. Cosmochim. Acta* 70:2006–22

Shen YA, Buick R, Canfield DE. 2001. Isotopic evidence for microbial sulphate reduction in the early Archaean era. *Nature* 410:77–81

Skulan JL, Beard BL, Johnson CM. 2002. Kinetic and equilibrium Fe isotope fractionation between aqueous Fe(III) and hematite. *Geochim. Cosmochim. Acta* 66:2995–3015

Staubwasser M, von Blanckenburg F, Schoenberg R. 2006. Iron isotopes in the early marine diagenetic iron cycle. *Geology* 34:629–32

Summons RE, Jahnke LL, Roksandic Z. 1994. Carbon isotopic fractionation in lipids from methanotrophic bacteria: relevance for interpretation of the geochemical record of biomarkers. *Geochim. Cosmochim. Acta* 58:2853–63

Sumner DY. 1997. Carbonate precipitation and oxygen stratification in Late Archean seawater as deduced from facies and stratigraphy of the Gamohaan and Frisco formations, Transvaal Supergroup, South Africa. *Am. J. Sci.* 297:455–87

Teutsch N, von Gunten U, Porcelli D, Cirpka OA, Halliday AN. 2005. Adsorption as a cause for iron isotope fractionation in reduced groundwater. *Geochim. Cosmochim. Acta* 69:4175–85

Thamdrup B, Canfield DE. 1996. Pathways of carbon oxidation in continental margin sediments off central Chile. *Limnol. Oceanogr.* 41:1629–50

Ueno Y, Yamada K, Yoshida N, Maruyama S, Isozacki Y. 2006. Evidence from fluid inclusions for microbial methanogenesis in the early Archean era. *Nature* 440:516–19

van Zullen MA, Lepland A, Arrhenius G. 2002. Reassessing the evidence for the earliest traces of life. *Nature* 418:627–30

Vargas M, Kashefi K, Blunt-Harris EL, Lovley DR. 1998. Microbiological evidence for Fe(III) reduction on early Earth. *Nature* 395:65–67

Walczyk T, von Blanckenburg F. 2002. Natural iron isotope variations in human blood. *Science* 295:2065–66

Welch SA, Beard BL, Johnson CM, Braterman PS. 2003. Kinetic and equilibrium Fe isotope fractionation between aqueous Fe(II) and Fe(III). *Geochim. Cosmochim. Acta* 67:4231–50

Whitehouse MJ, Fedo CM. 2007. Microscale heterogeneity of Fe isotopes in >3.71 Ga banded iron formation from the Isua Greenstone Belt, southwest Greenland. *Geology* 35:719–22

Widdel F, Schnell S, Heising S, Ehrenreich A, Assmus B, Schink B. 1993. Ferrous iron oxidation by anoxygenic phototrophic bacteria. *Nature* 362:834–36

Wiederhold JG, Kraemer SM, Teutsch N, Borer PM, Halliday AN, Kretzschmar R. 2006. Iron isotope fractionation during proton-promoted, ligand-controlled, and reductive dissolution of goethite. *Environ. Sci. Technol.* 40:3787–93

Wiesli RA, Beard BL, Johnson CM. 2004. Experimental determination of Fe isotope fractionation between aqueous Fe(II), siderite and "green rust" in abiotic systems. *Chem. Geol.* 211:343–62

Wille M, Kramers JD, Nagler TF, Beukes NJ, Schroder S, et al. 2007. Evidence for a gradual rise of oxygen between 2.6 and 2.5 Ga from Mo isotopes and Re-PGE signatures in shales. *Geochim. Cosmochim. Acta* 71:2417–35

Williams AGB, Scherer MM. 2004. Spectroscopic evidence for Fe(II)-Fe(III) electron transfer at the Fe oxide-water interface. *Environ. Sci. Technol.* 38:4782–90

Xiong J, Fischer WM, Inoue K, Nakahara M, Bauer CE. 2000. Molecular evidence for the early evolution of photosynthesis. *Science* 289:1724–30

Yamaguchi KE, Johnson CM, Beard BL, Ohmoto H. 2005. Biogeochemical cycling of iron in the Archean-Paleoproterozoic Earth: constraints from iron isotope variations in sedimentary rocks from the Kaapvaal and Pilbara Cratons. *Chem. Geol.* 218:135–69

Zerkle AL, House CH, Brantley SL. 2005. Biogeochemical signatures through time as inferred from whole microbial genomes. *Am. J. Sci.* 305:467–502

Annual Review
of Earth and
Planetary Sciences
Volume 36, 2008

Contents

Frontispiece
Margaret Galland Kivelson xii

The Rest of the Solar System
Margaret Galland Kivelson 1

Abrupt Climate Changes: How Freshening of the Northern Atlantic Affects the Thermohaline and Wind-Driven Oceanic Circulations
Marcelo Barreiro, Alexey Fedorov, Ronald Pacanowski, and S. George Philander 33

Geodynamic Significance of Seismic Anisotropy of the Upper Mantle: New Insights from Laboratory Studies
Shun-ichiro Karato, Haemyeong Jung, Ikuo Katayama, and Philip Skemer 59

The History and Nature of Wind Erosion in Deserts
Andrew S. Goudie 97

Groundwater Age and Groundwater Age Dating
Craig M. Bethke and Thomas M. Johnson 121

Diffusion in Solid Silicates: A Tool to Track Timescales of Processes Comes of Age
Sumit Chakraborty 153

Spacecraft Observations of the Martian Atmosphere
Michael D. Smith 191

Crinoid Ecological Morphology
Tomasz K. Baumiller 221

Oceanic Euxinia in Earth History: Causes and Consequences
Katja M. Meyer and Lee R. Kump 251

The Basement of the Central Andes: The Arequipa and Related Terranes
Victor A. Ramos 289

Modeling the Dynamics of Subducting Slabs
Magali I. Billen 325

Geology and Evolution of the Southern Dead Sea Fault with Emphasis on Subsurface Structure
Zvi Ben-Avraham, Zvi Garfunkel, and Michael Lazar 357

The Redox State of Earth's Mantle
Daniel J. Frost and Catherine A. McCammon 389

The Seismic Structure and Dynamics of the Mantle Wedge
Douglas A. Wiens, James A. Conder, and Ulrich H. Faul 421

The Iron Isotope Fingerprints of Redox and Biogeochemical Cycling in the Modern and Ancient Earth
Clark M. Johnson, Brian L. Beard, and Eric E. Roden 457

The Cordilleran Ribbon Continent of North America
Stephen T. Johnston 495

Rheology of the Lower Crust and Upper Mantle: Evidence from Rock Mechanics, Geodesy, and Field Observations
Roland Bürgmann and Georg Dresen 531

The Postperovskite Transition
Sang-Heon Shim 569

Coastal Impacts Due to Sea-Level Rise
Duncan M. FitzGerald, Michael S. Fenster, Britt A. Argow, and Ilya V. Buynevich 601

Indexes

Cumulative Index of Contributing Authors, Volumes 26–36 649

Cumulative Index of Chapter Titles, Volumes 26–36 653

Errata

An online log of corrections to *Annual Review of Earth and Planetary Sciences* articles may be found at http://earth.annualreviews.org